RESEARCH ARTICLE

Figures and figure supplements

Convergent organization of aberrant MYB complex controls oncogenic gene expression in acute myeloid leukemia

Sumiko Takao *et al*

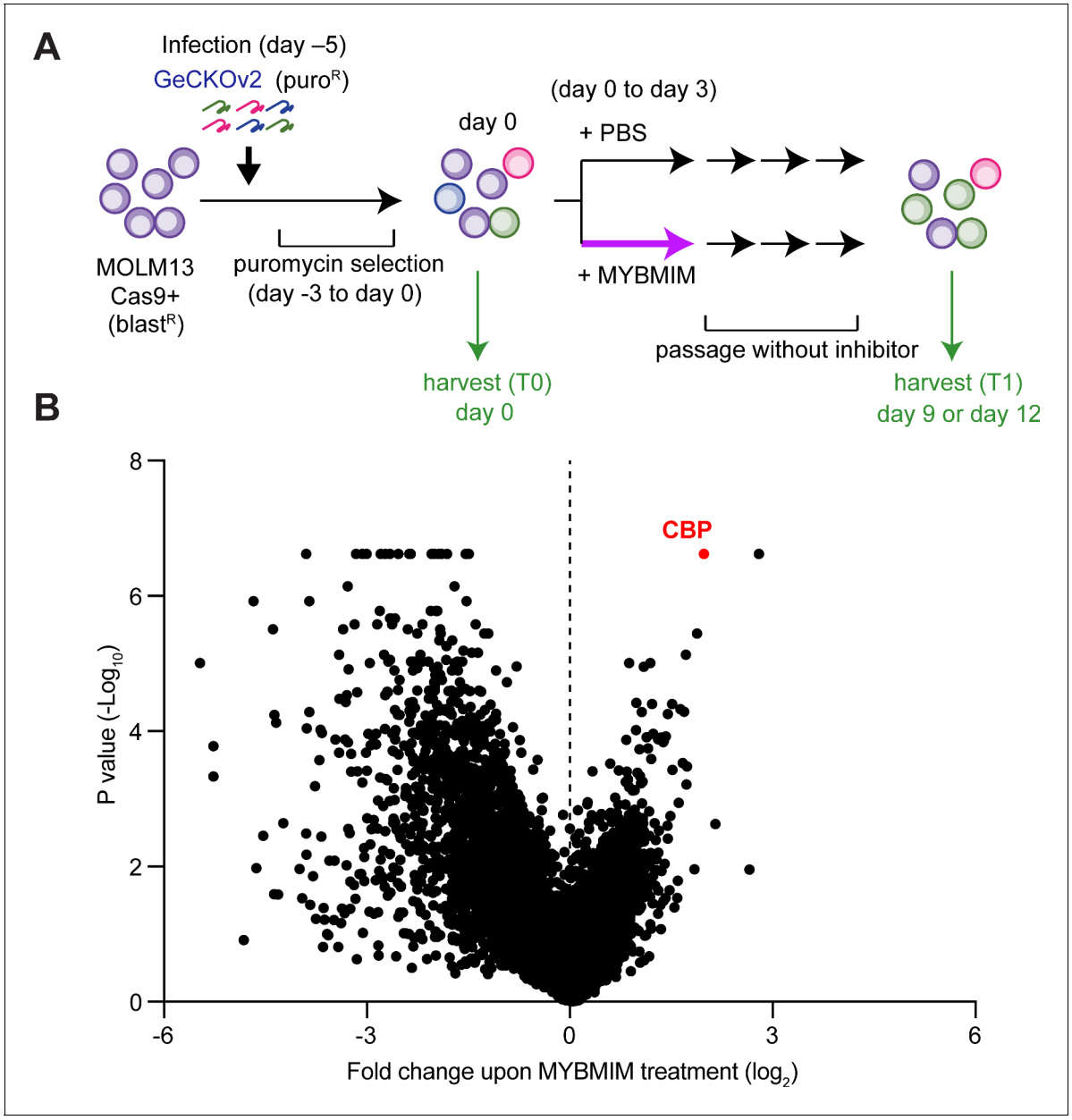

Figure 1. CBP depletion is required to confer resistance to MYBMIM in AML cells. (**A**) Schematic of the genome-wide CRISPR screen to identify genes whose loss modifies MYBMIM effects in MOLM13 cells expressing Cas9. Cells were transduced with the GeCKOv2 library expressing single sgRNAs at low multiplicity of infection, followed by 3-day treatment with 10 μM MYBMIM versus PBS control, with the sgRNA representation assessed by DNA sequencing. (**B**) Volcano plot showing the relative abundance of cell clones expressing sgRNAs targeting specific genes (fold change of MYBMIM-treated cells at T1 versus T0) and their statistical significance from biological replicates. Dashed line represents no enrichment, with positive values representing genes whose depletion confers relative resistance to MYBMIM. CBP is marked in red.

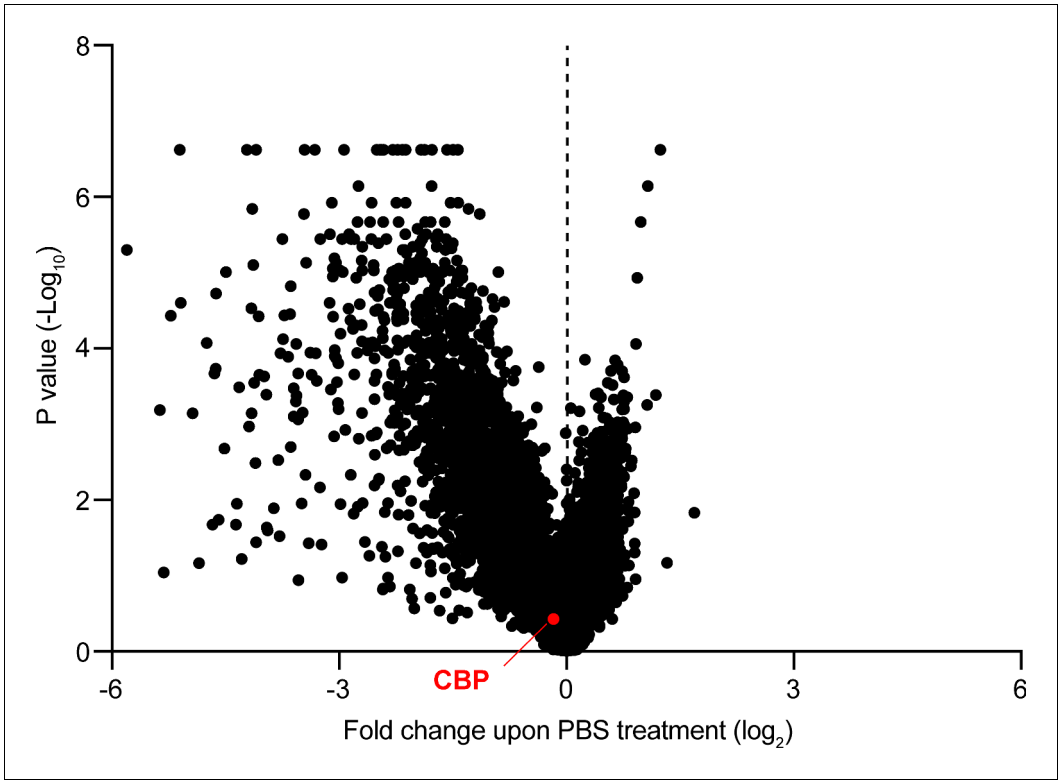

Figure 1—figure supplement 1. CBP depletion is dispensable in AML cells. Volcano plot showing the relative abundance of MOLM13-Cas9 cell clones expressing sgRNAs targeting specific genes (fold change of PBS-treated cells at T1 versus T0) and their statistical significance from biological replicates. Dashed line represents no enrichment, with positive values representing genes whose depletion confers relative resistance to MYBMIM. CBP is marked in red.

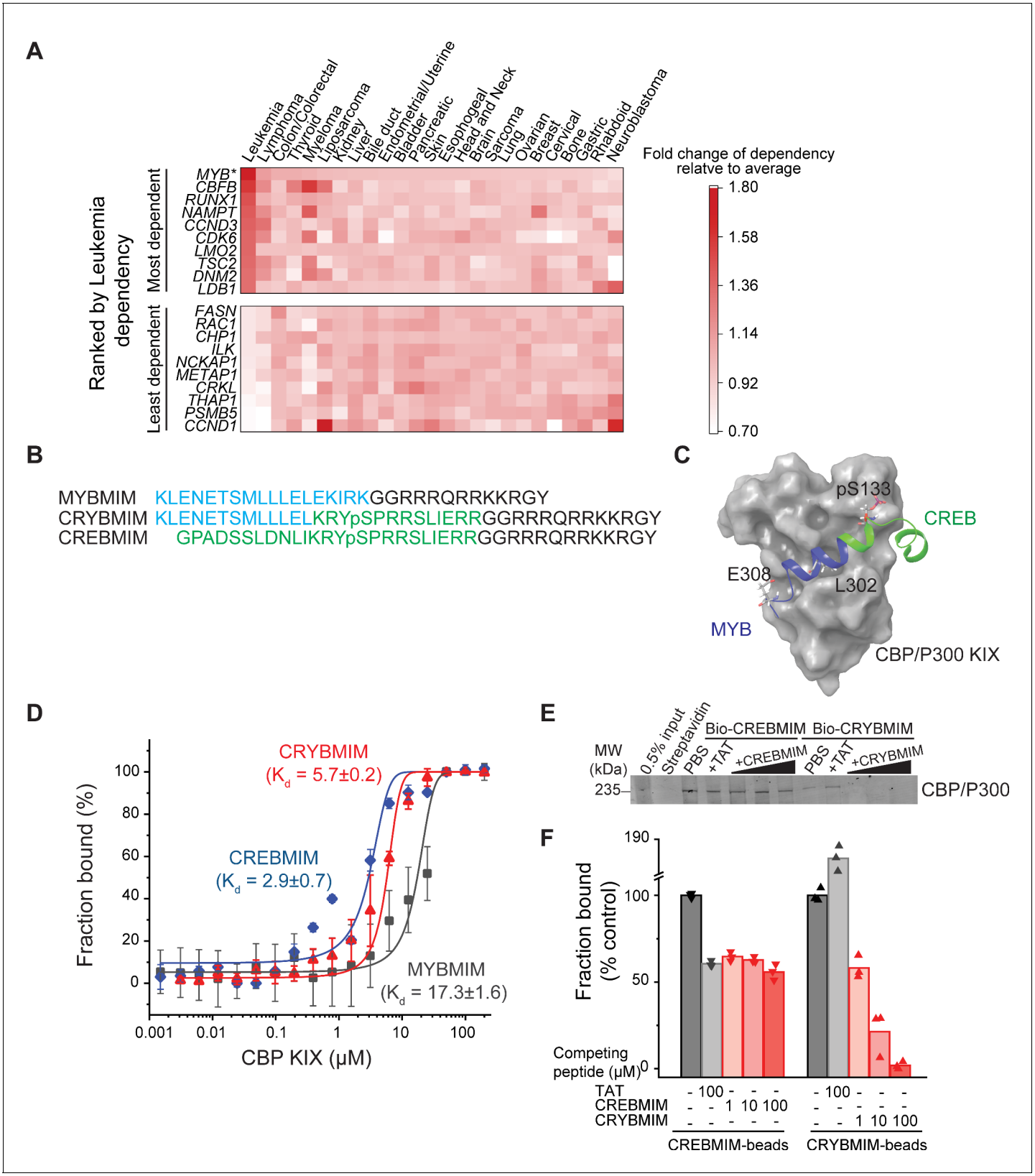

Figure 2. CRYBMIM is an improved peptidomimetic chimera that specifically binds the KIX domain of CBP/P300 in vitro and in cells. (**A**) Heatmap of the top 10 and bottom 10 gene dependencies for survival and proliferation of 652 cancer cell lines in the DepMap Cancer Dependency Map Project, ranked by the greatest dependency for 37 leukemia lines, 20 of which are AML cell lines, as indicated by the red color gradient; *p=1.1e-15, t-test of

Figure 2 continued on next page

Figure 2 continued

leukemia versus other tumor types. (**B**) Retro-inverso amino acid sequences of MYBMIM, CREBMIM and CRYBMIM, with amino acids derived from MYB, CREB, and TAT marked in blue, green, and black, respectively. (**C**) Molecular model of the CRYBMIM:KIX complex. Residues making contact with KIX are labeled, with portions derived from MYB and CREB marked in blue and green, respectively. (**D**) Binding of FITC-conjugated CREBMIM (blue), CRYBMIM (red), and MYBMIM (black), as measured using microscale thermophoresis; K_d = 2.9 ± 0.7, 5.7 ± 0.2, and 17.3 ± 1.6, respectively. Error bars represent standard deviations of three biological replicates; p<1e-15, ANOVA, for CRYBMIM versus MYBMIM. (**E**) Western blot showing binding of nuclear CBP/P300 isolated from AML cells to biotinylated CRYBMIM or CREBMIM, specifically competed by the excess free peptides as indicated. (**F**) Quantification of CBP/P300 binding to CRYBMIM and CREBMIM by fluorescence densitometry, with black, gray, and red denoting PBS control, TAT control, and peptide competition, respectively.

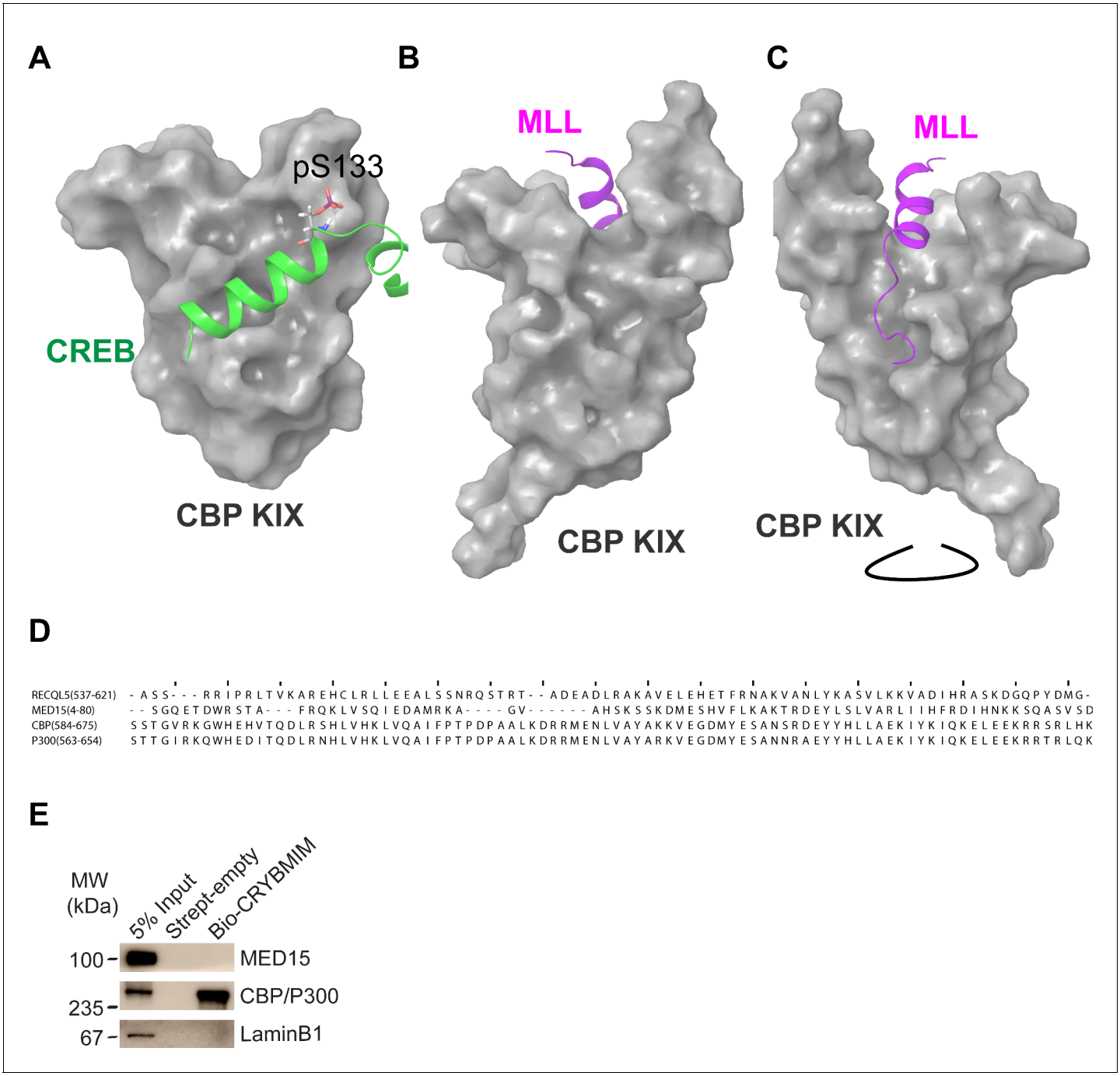

Figure 2—figure supplement 1. Molecular models of CREB and MLL structures in complex with CBP KIX, and CRYBMIM selectively binds to KIX domain in CBP/P300. (**A**) Molecular model of the CREB:KIX complex assembled in Maestro (Schrödinger) using PDB 1KDX showing phosphor-Serine 133. (**B**) Molecular model of the MLL:KIX complex assembled in Maestro (Schrödinger) using PDB 2LXS shown from the MYB/CREB binding site on KIX. (**C**) Molecular model of the MLL:KIX complex assembled in Maestro (Schrödinger) using PDB 2LXS rotated to show the full MLL peptide. (**D**) Sequence alignment of KIX domains in different human proteins. Identity/similarity of each set of sequences were 88%/96% (CBP vs P300), 21%/38% (CBP vs MED15), and 17%/34% (CBP vs RECQL5). (**E**) Western blots following affinity purification of MV411 nuclear extracts, showing specific binding of CBP/P300 but not MED15 to biotinylated CRYBMIM (Bio-CRYBMIM), immobilized on streptavidin beads. Purification with beads alone (Strept-empty) and LaminB1 serve as specificity controls.

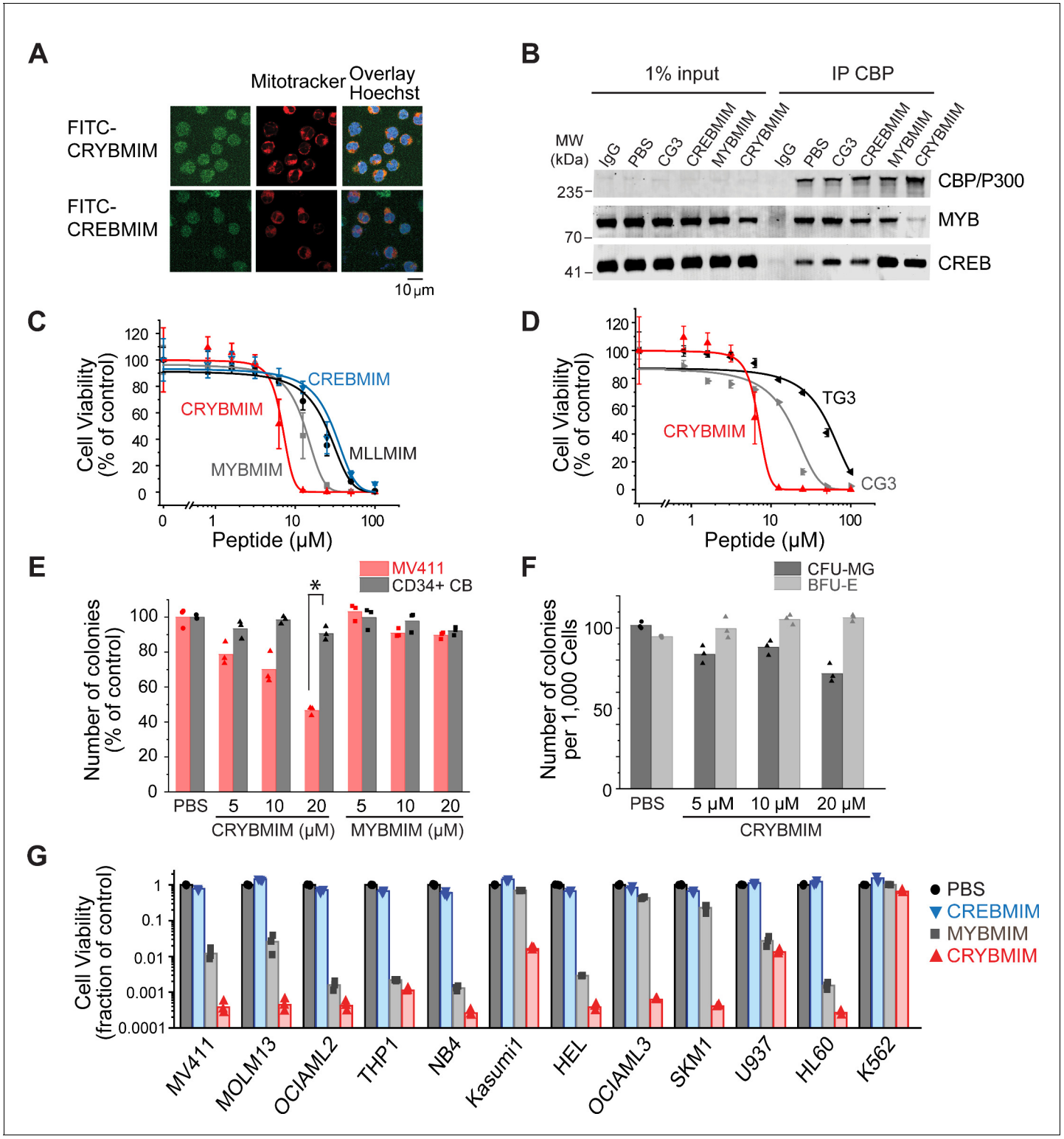

Figure 3. Potent and broad-spectrum activity of CRYBMIM against diverse AML cell lines but relatively sparing of normal hematopoietic progenitor cells. (**A**) Representative live cell confocal microscopy images of MV411 cells treated with 100 nM FITC-conjugated peptides as indicated for 1 hr, counterstained with Mitotracker (red) and Hoechst 33342 (blue). Scale bar indicates 20 µm, with z-stack of 1.5 µm. (**B**) Western blots showing immunoprecipitated nuclear CBP/P300 co-purified with MYB and CREB from MV411 cells treated with 10 µM peptides as indicated for 1 hr. (**C–D**) Cell viability of MV411 cells as a function of increasing concentrations of 48 hr peptide treatment, comparing (**C**) CRYBMIM to MYBMIM, CREBMIM and MLLMIM (IC_{50} = 6.88 ± 3.39, 13.1 ± 3.3 29.15 ± 3.79, and 24.22 ± 2.00, p<1e-15, ANOVA); (**D**) TG3 and CG3 (IC_{50} = 16.65 ± 1.00 and 48.91 ± 2.55, p<1e-

Figure 3 continued on next page

Figure 3 continued

15, ANOVA). Error bars represent standard deviation of three biological replicates. (**E**) Colony forming ability of CD34+ cells isolated from human umbilical cord blood (CD34+ CB, gray) and MV411 AML (red) cells following CRYBMIM or MYBMIM treatment. Data represent three biological replicates; *p=7.4e-5, t-test of normal CD34+ CB versus MV411 AML cells. (**F**) Preservation of clonogenic capacity of CD34+ CB cells in differentiating into erythroid blast forming units (BFU-E, light gray) and granulocyte macrophage colony forming units (CFU-GM, gray) as a function of CRYBMIM treatment. (**G**) Cell viability of AML cell lines treated with control PBS (black), 20 μM CREBMIM (blue), MYBMIM (gray), or CRYBMIM (red) as indicated for 6 days with media replacement every 48 hr in three biological replicates (p=8.6e-3, t-test for CRYBMIM versus control).

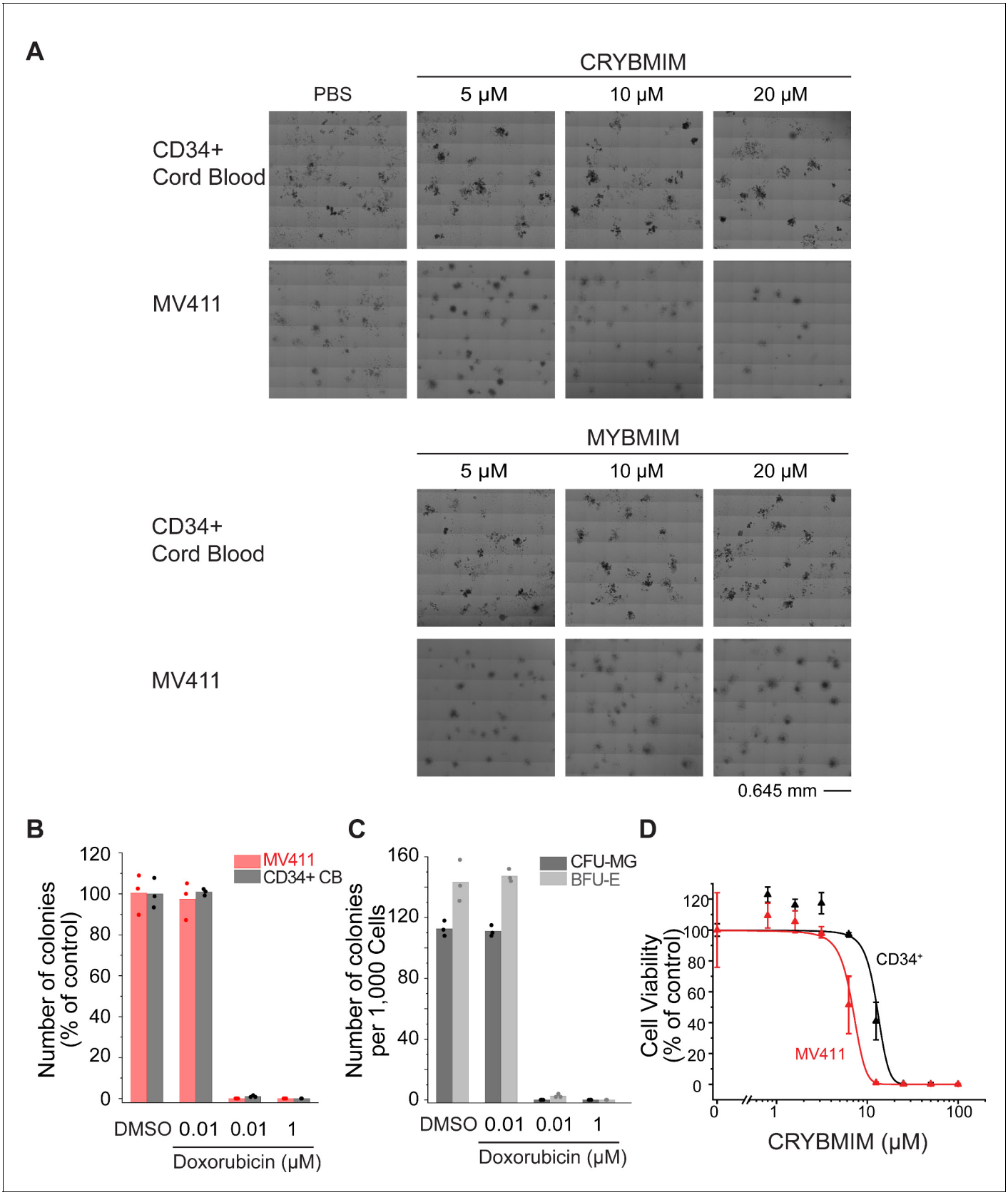

Figure 3—figure supplement 1. CRYBMIM relatively spares normal hematopoietic progenitor cells in vitro. (**A**) Phase contrast photographs of MV411 and CD34+ cells isolated from human umbilical cord blood (CD34+ CB) and cultured in MethoCult H3040 with drug treatment, as indicated. (**B**) Colony

Figure 3—figure supplement 1 continued on next page

Figure 3—figure supplement 1 continued

forming ability of MV411 and CD34+ CB cells cultured in MethoCult H3040 following doxorubicin treatment. (**C**) Formation of BFU-E (light gray) and CFU-GM (gray) colonies of CD34+ CB cells cultured in MethoCult H3040 upon doxorubicin treatment. (**D**) Growth of MV411 and CD34+ CB cells upon CRYBMIM treatment in serum-containing suspension culture (IC_{50} = 6.9 ± 3.4 vs 13 ± 3.6 μM, p=1.1e-15, ANOVA). Symbols represent biological triplicates.

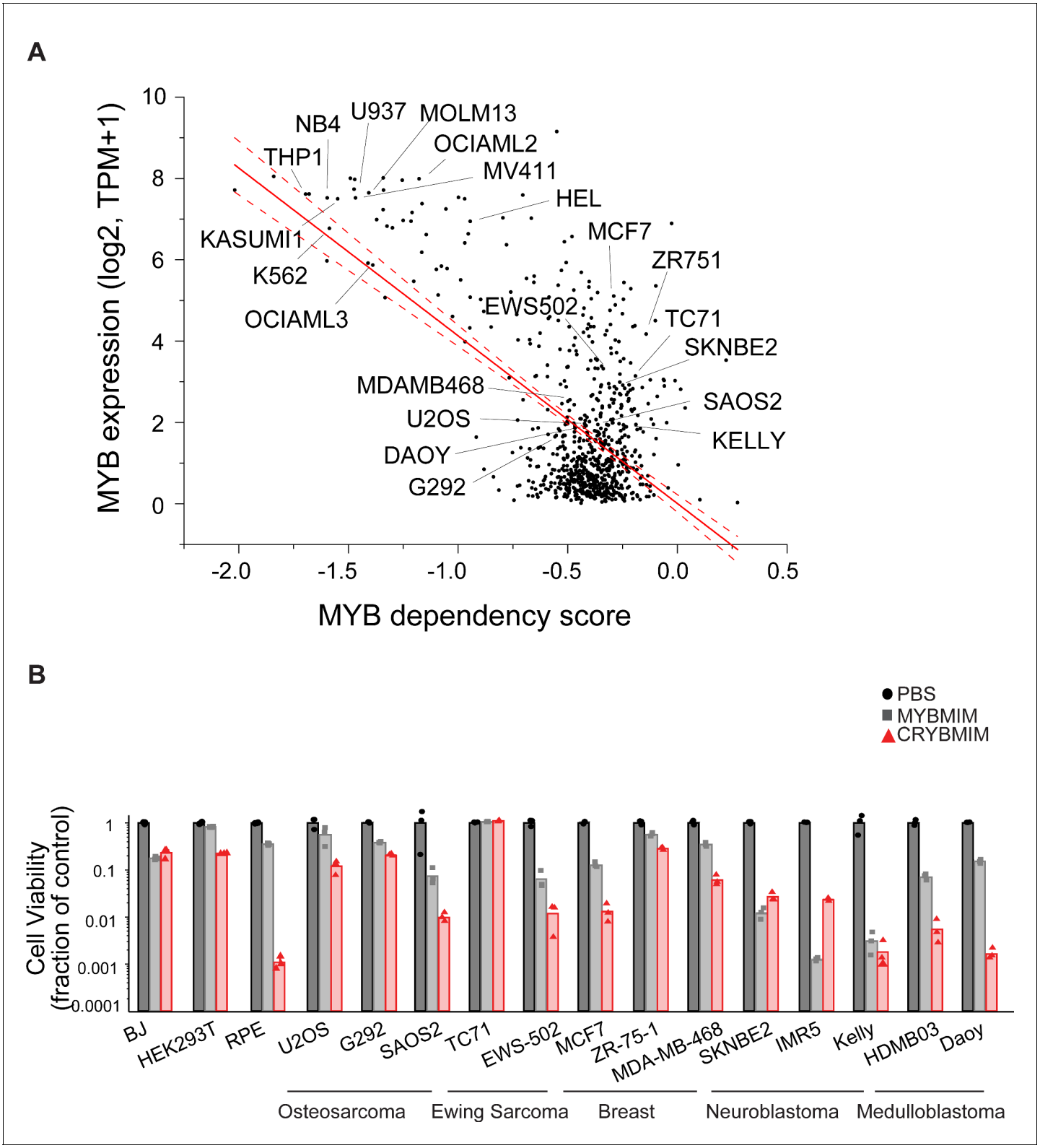

Figure 3—figure supplement 2. Activity of CRYBMIM on non-hematopoietic cells. (**A**) Expression of MYB as a function of its genetic dependency in tumor cell lines, as assessed by DepMap. Red line represents linear correlation, with dashed lines showing 95% confidence intervals. (**B**) Cell viability assays of non-leukemia tumor and non-tumor cell lines treated with control PBS (black), 20 μM MYBMIM (gray), or 20 μM CRYBMIM (red) as indicated for 6 days with media replacement every 48 hr in three biological replicates.

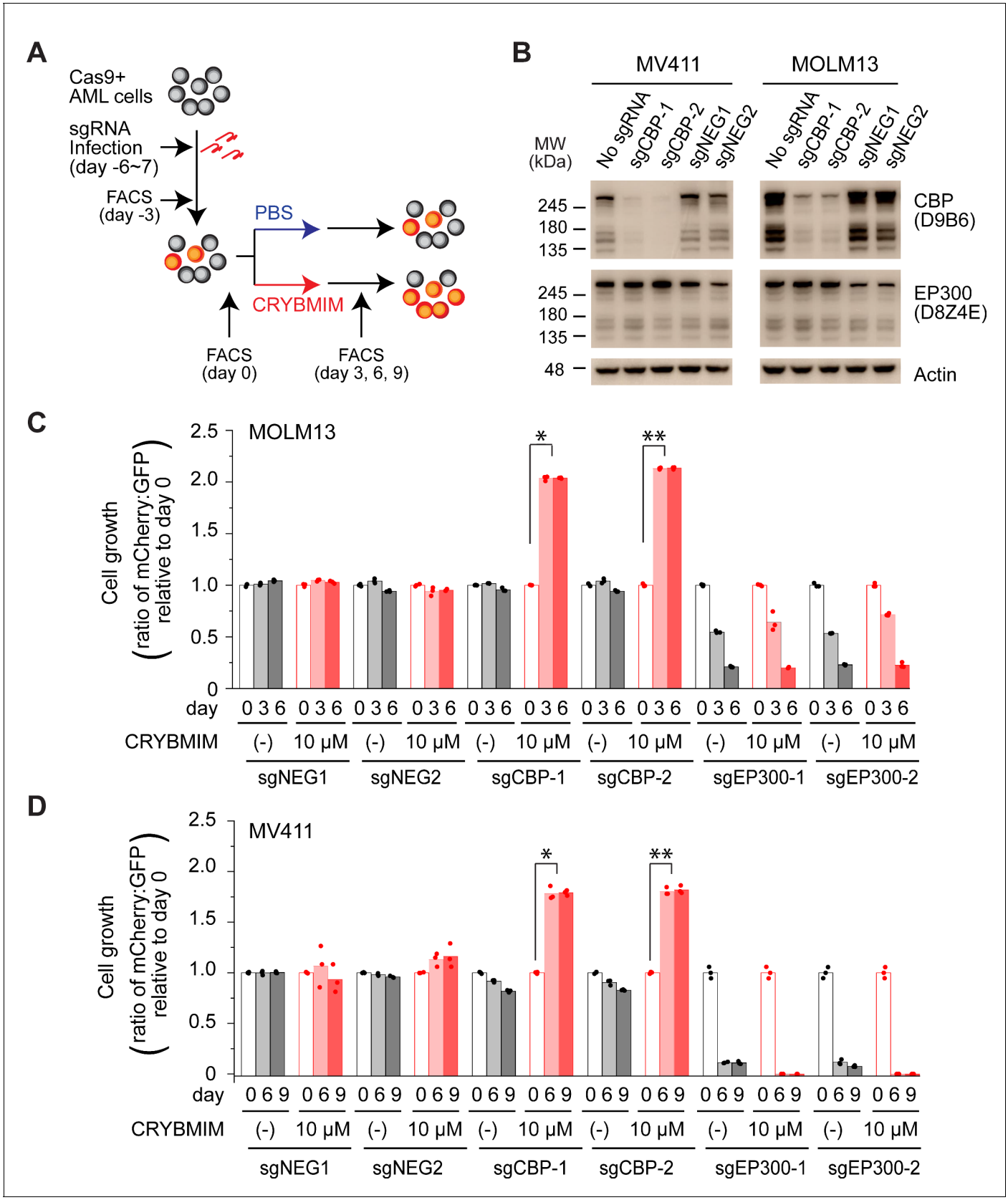

Figure 4. CBP but not P300 is dispensable for the growth and survival of AML cells, and is required for the susceptibility to peptidomimetic MYB blockade by CRYBMIM. (**A**) Schematic of the competitive assays to define specific genetic dependencies. AML cells expressing Cas9 and GFP are

Figure 4 continued on next page

Figure 4 continued

transduced with sgRNAs targeting specific genes and expressing mCherry, followed by quantitation of cell abundance by fluorescence activated cell scanning (FACS) of GFP and mCherry-expressing cells. (**B**) Western blots demonstrating specific depletion of CBP in MV411 (left) and MOLM13 (right) cells expressing sgCBP-1 and sgCBP-2, as compared to control sgNEG1 and sgNEG2 targeting the *AAVS1* safe harbor locus. EP300 is shown for specificity, and Actin serves as the loading control. (**C**) Relative growth of GFP-expressing MOLM13 cells expressing mCherry and unique sgRNAs targeting *AAVS1* control (sgNEG1 and sgNEG2), *CBP* (sgCBP-1 and sgCBP-2), and *P300* (sgEP300-1 and sgEP300-2) and quantified by FACS on day 0, 3, and 6 after 2-day treatment with 10 μM CRYBMIM or PBS. Data represent biological triplicates of at least 10,000 cells per condition; *p=6.0e-10, **p=4.1e-8, t-test for day 6 versus day 0 of CRYBMIM treatment of CBP-depleted cells. (**D**) Analogous experiment as (**C**) using MV411 cells; *p=1.1e-6, **p=3.7e-6, t-test for day 6 versus day 0 of CRYBMIM treatment of CBP-depleted cells.

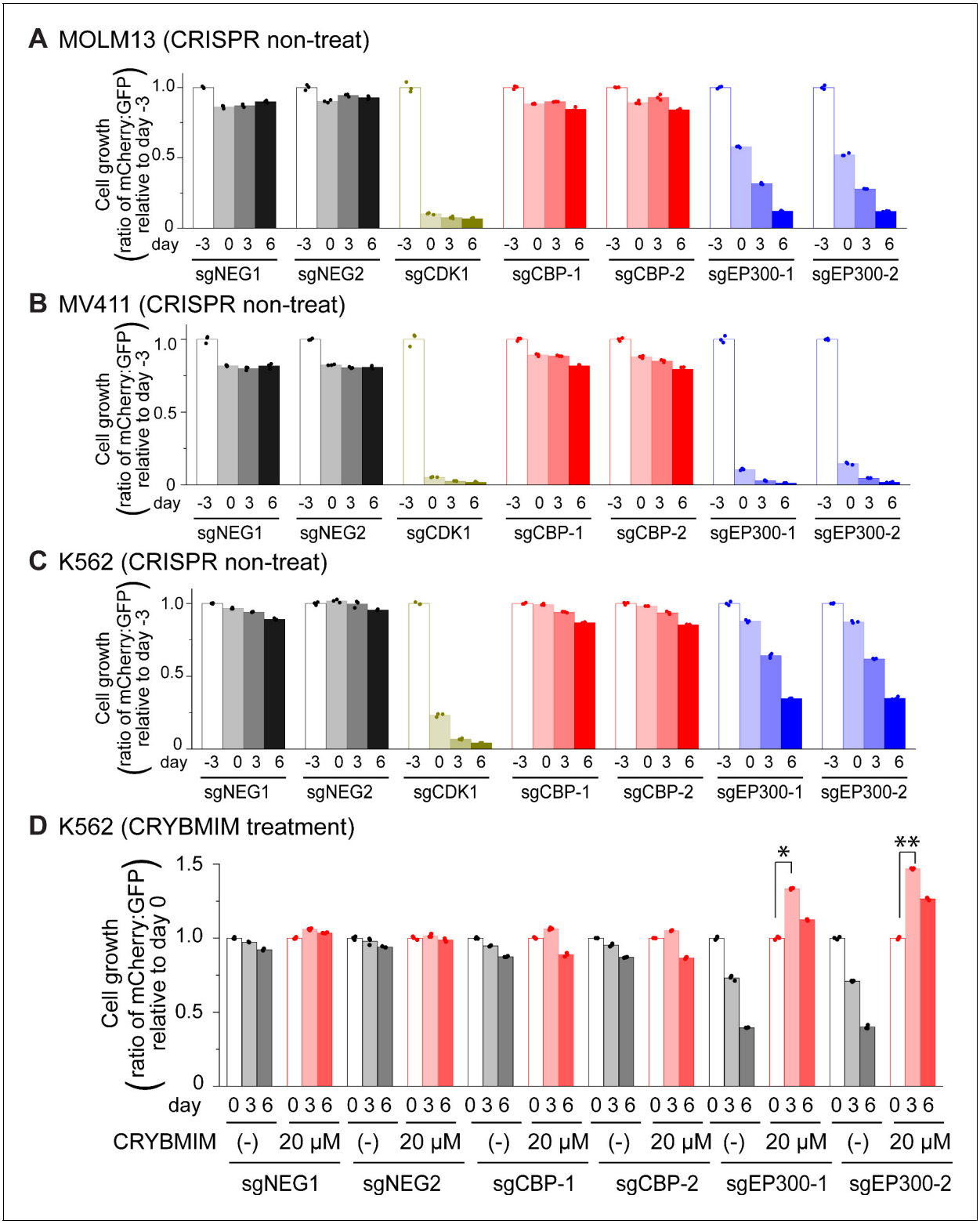

Figure 4—figure supplement 1. Genetic dependencies of CRYBMIM susceptibility in AML cells. (**A–C**) Relative growth of GFP-expressing MOLM13 (**A**), MV411 (**B**), and K562 (**C**) cells expressing mCherry and unique sgRNAs targeting negative control *AAVS1* (sgNEG1 and sgNEG2), positive control *CDK1* (sgCDK1), *CBP* (sgCBP-1 and sgCBP-2), and *P300* (sgEP300-1 and sgEP300-2) and quantified by FACS on days –3, 0, 3, and 6 upon sgRNA transduction. (**D**) Relative growth of K562-Cas9 cells expressing specific sgRNAs upon treatment with 20 μM CRYBMIM for 2 days (*p=1.0e-6, **p=1.3e-7; t-test for day 3 versus day 0).

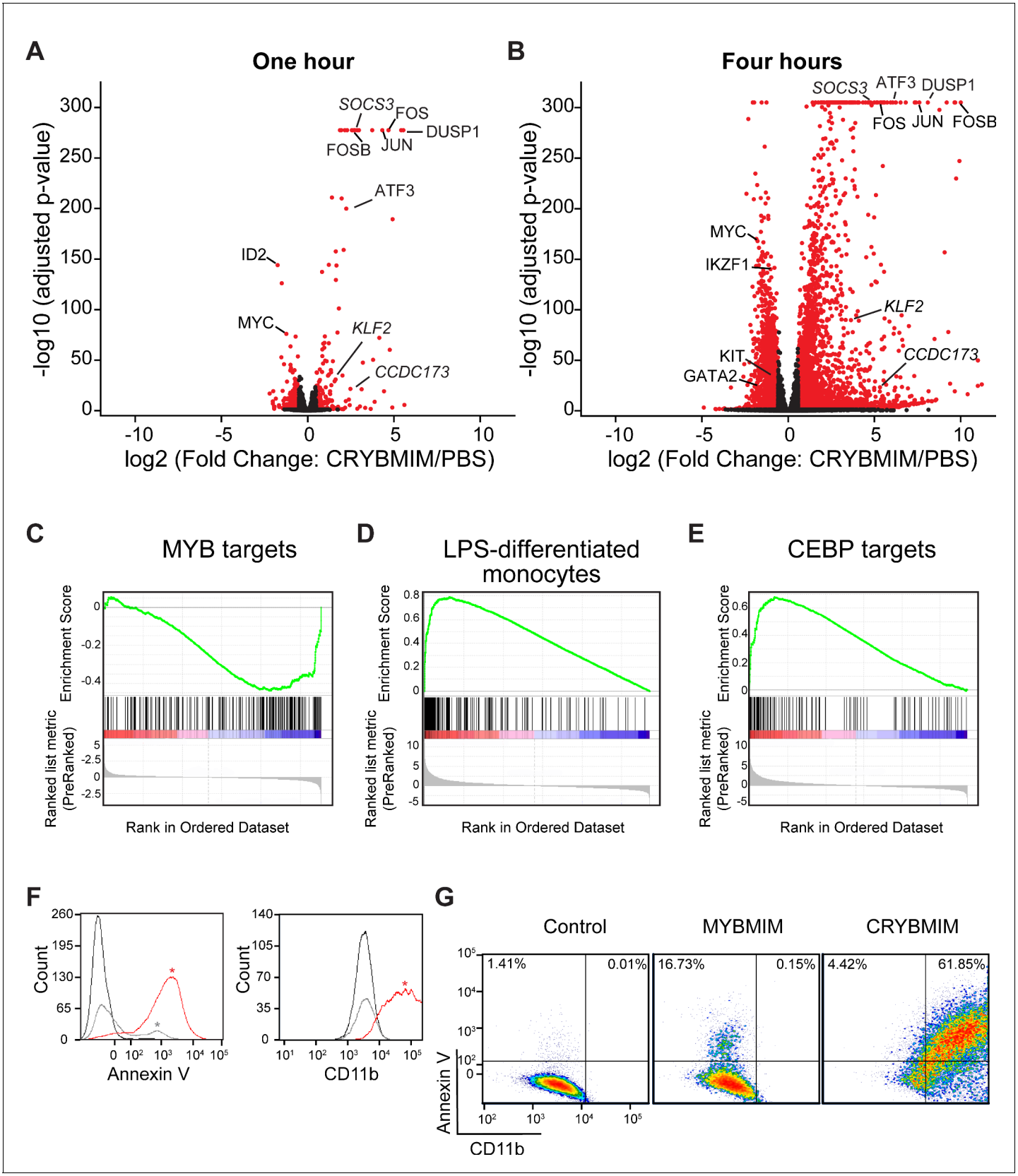

Figure 5. CRYBMIM blocks oncogenic MYB gene expression and restores normal myeloid cell differentiation. (**A–B**) Volcano plots of normalized gene expression of MV411 cells upon one (**A**) and four hour (**B**) treatment with CRYBMIM, as compared to PBS control, with select genes labeled; p-values

Figure 5 continued on next page

Figure 5 continued

denote statistical significance of three biological replicates. (**C–E**) Gene set enrichment analysis of up- and downregulated gene sets: (**C**) MYB_Q6, (**D**) GSE9988_LPS_VS_VEHICLE_TREATED_MONOCYTES_UP, and (**E**) GERY_CEBP_TARGETS_377. (**F**) Histogram of Annexin V- or CD11b-stained MV411 cell fluorescence, treated with CRYBMIM (red), MYBMIM (gray), or control PBS (black); *p<1e-15, Kruskal-Wallis test. (**G**) Scatter plots comparing Annexin V- versus CD11b-stained MV411 cell fluorescence, treated with control PBS, MYBMIM or CRYBMIM; blue to red color indicates increasing cell density.

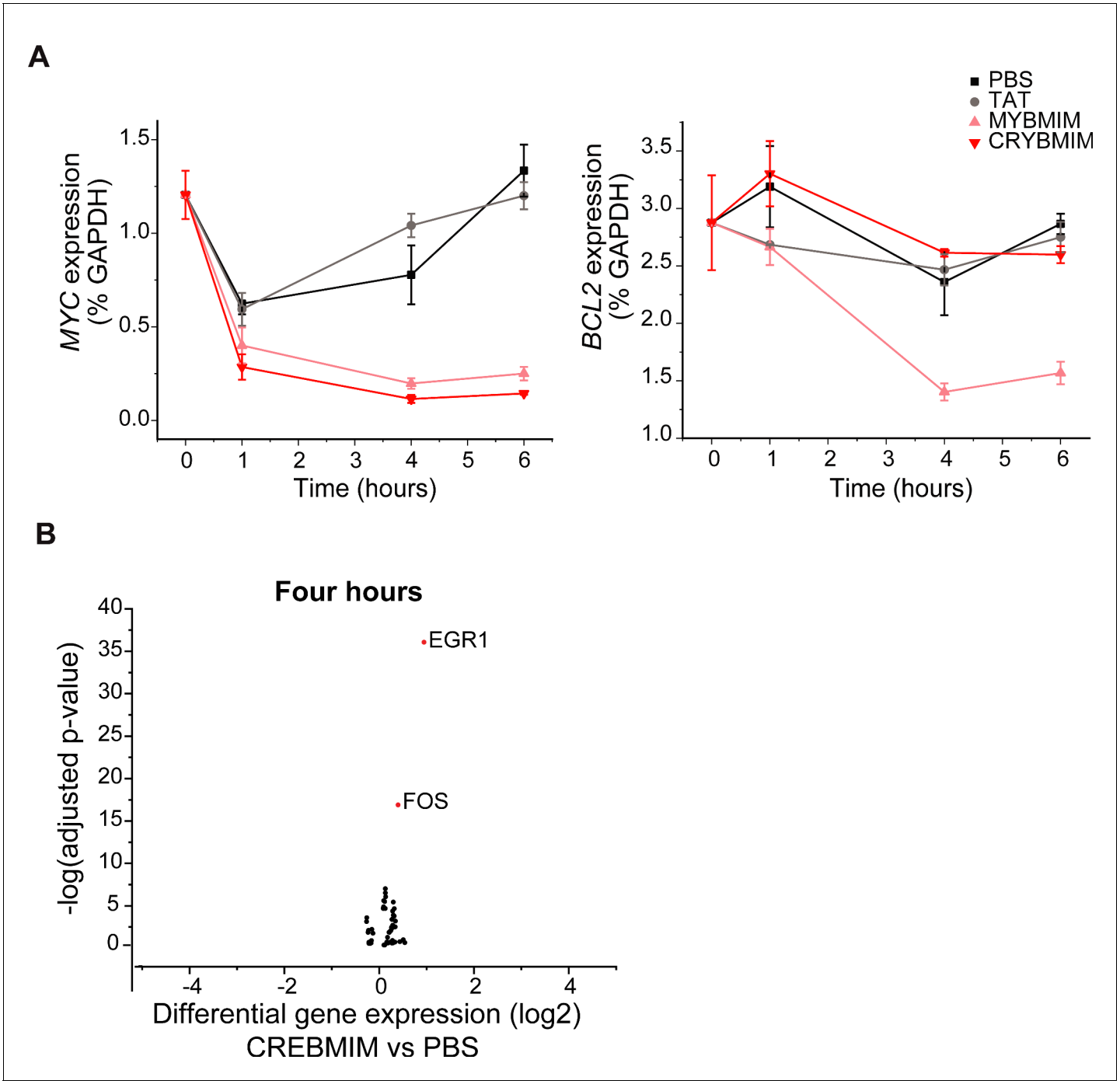

Figure 5—figure supplement 1. CRYBMIM but not CREBMIM causes significant changes in gene expression in AML cells upon short duration exposure. (**A–B**) Gene expression of MYB target genes *MYC* (**A**) and *BCL2* (**B**) in AML after 20 µM peptide treatment as measured by qPCR. (**C**) Gene expression changes in MV411 cells treated with 20 µM CREBMIM for 4 hr as measured by RNA-seq.

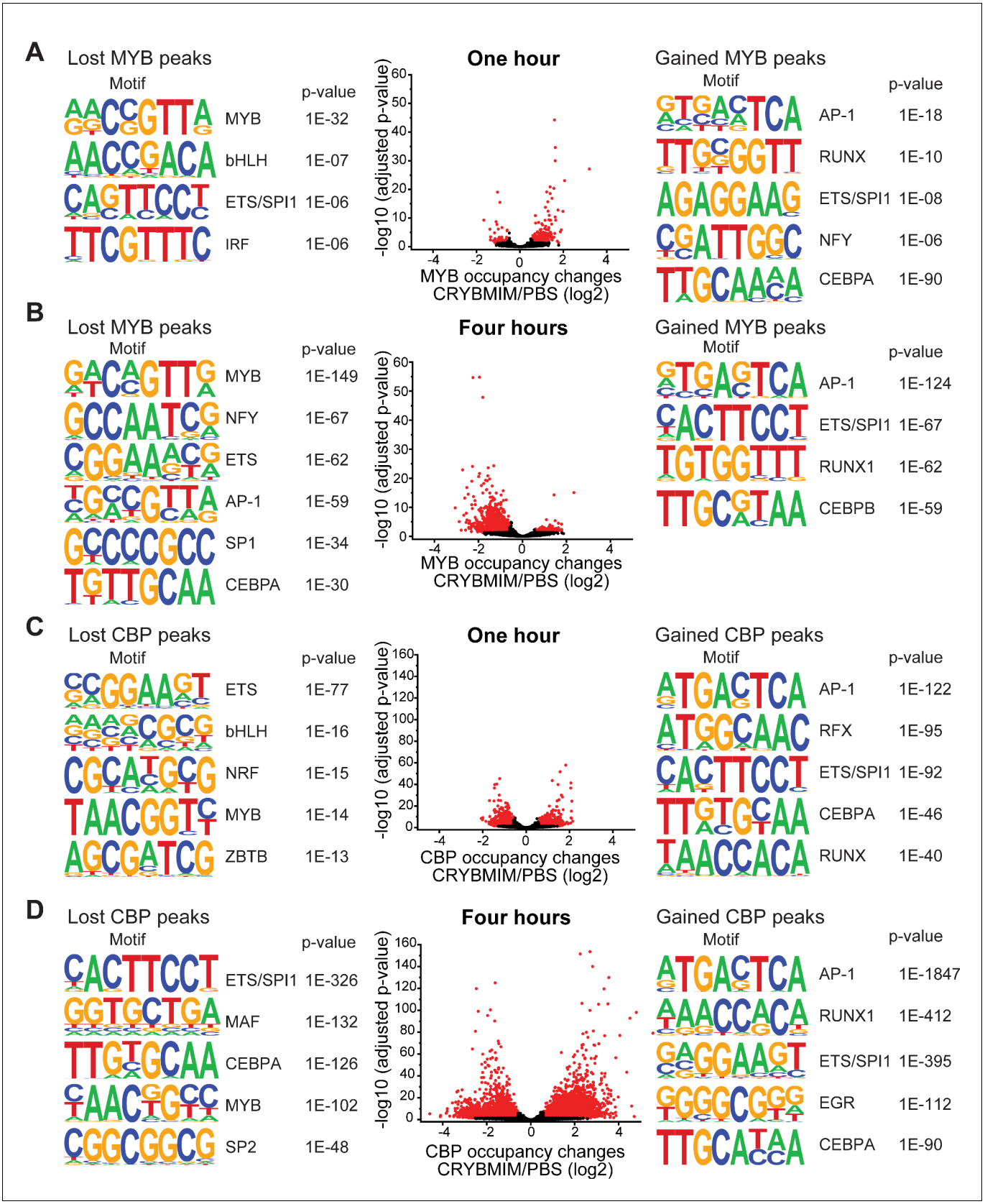

Figure 6. CRYBMIM remodels MYB and CBP/P300 chromatin complexes in AML cells. (**A–B**) Volcano plots of relative MYB chromatin occupancy in MV411 cells changes after 1 hr (**A**) and 4 hr (**B**) of 20 µM CRYBMIM treatment compared to PBS control, as analyzed by ChIP-seq. Sequence motifs

Figure 6 continued on next page

Figure 6 continued

found in CRYBMIM-induced MYB-depleted (left) and MYB-enriched loci (right) are shown. p-Values denote statistical significance of three technical replicates. (**C–D**) Volcano plots of CBP/P300 chromatin occupancy changes after 1 hr (**C**) and 4 hr (**D**) of 20 μM CRYBMIM treatment as compared to control, as analyzed by ChIP-seq. Sequence motifs found in CRYBMIM-induced CBP/P300-depleted (left) and CBP/P300-enriched loci (right) are shown. p-Values denote statistical significance of three technical replicates.

A

One hour

Lost MYB peaks

Rank	Motif	P-value	log P-pvalue	% of Targets	% of Background	STD(Bg STD)	Best Match/Details
1		1e-32	-7.510e+01	52.50%	9.24%	332.1bp (335.2bp)	BMYB(HTH)/Hela-BMYB-ChIP-Seq(GSE27030)/Homer(0.927)
2 *		1e-7	-1.700e+01	46.67%	23.85%	534.5bp (319.5bp)	bHLH10(bHLH)/colamp-bHLH10-DAP-Seq(GSE60143)/Homer(0.919)
3 *		1e-6	-1.474e+01	55.00%	32.68%	687.7bp (322.1bp)	PU.1(ETS)/ThioMac-PU.1-ChIP-Sc (GSE21512)/Homer(0.851)
4 *		1e-6	-1.400e+01	12.50%	2.67%	650.5bp (340.1bp)	T1ISRE(IRF)/ThioMac-Ifnb-Expression/Homer(0.810)

Gained MYB peaks

Rank	Motif	P-value	log P-pvalue	% of Targets	% of Background	STD(Bg STD)	Best Match/Details
1		1e-18	-4.195e+01	23.36%	7.45%	711.5bp (404.5bp)	AP-1(bZIP)/ThioMac-PU.1-ChIP-Seq(GSE21512)/Homer(0.894)
2 *		1e-10	-2.437e+01	25.55%	12.03%	571.1bp (484.0bp)	RUNX2/MA0511.2/Jaspar(0.949)
3 *		1e-8	-1.935e+01	32.40%	18.76%	561.5bp (475.6bp)	SPIB/MA0081.1/Jaspar(0.873)
4 *		1e-6	-1.605e+01	28.35%	16.62%	593.4bp (522.8bp)	NFY(CCAAT)/Promoter/Homer(0.914)
5 *		1e-6	-1.530e+01	27.10%	15.88%	555.4bp (440.4bp)	CEBP:AP1(bZIP)/ThioMac-CEBPb-ChIP-Seq(GSE21512)/Homer(0.890)
6 *		1e-5	-1.362e+01	66.36%	53.22%	697.6bp (474.6bp)	Myog/MA0500.1/Jaspar(0.934)
7 *		1e-4	-1.095e+01	26.17%	16.87%	591.2bp (470.5bp)	Rfx1(HTH)/NPC-H3K4me1-ChIP-Seq(GSE16256)/Homer(0.780)
8 *		1e-4	-9.771e+00	18.69%	11.23%	669.5bp (399.4bp)	At5g04390(C2H2)/col200-At5g04390-DAP-Seq(GSE60143)/Homer(0.822)
9 *		1e-3	-7.159e+00	3.12%	0.90%	248.1bp (583.3bp)	OPI1/Literature(Harbison)/Yeast(0.701)
10 *		1e-1	-4.294e+00	30.84%	25.24%	559.6bp (686.6bp)	Sp5(Zf)/mES-Sp5.Flag-ChIP-Seq(GSE72989)/Homer(0.807)
11 *		1e-1	-3.857e+00	4.36%	2.35%	505.6bp (680.1bp)	ACE2/ACE2_YPD/2-SWI5(Harbison)/Yeast(0.840)
12 *		1e0	-6.503e-01	9.35%	9.32%	453.4bp (413.2bp)	ZCRB1(RRM)/Homo_sapiens-RNCMPT00087-PBM/HughesRNA(0.814)
13 *		1e0	-3.934e-02	0.93%	2.06%	307.4bp (428.8bp)	ZEB1(Zf)/PDAC-ZEB1-ChIP-Seq(GSE64557)/Homer(0.770)

* possible false positive

B

Four hour

Lost MYB peaks

Rank	Motif	P-value	log P-pvalue	% of Targets	% of Background	STD(Bg STD)	Best Match/Details
1		1e-149	-3.454e+02	55.95%	31.63%	709.7bp (502.7bp)	MYB77(MYB)/col-MYB77-DAP-Seq(GSE60143)/Homer(0.918)
2		1e-67	-1.566e+02	27.30%	14.36%	683.7bp (686.8bp)	NFY(CCAAT)/Promoter/Homer(0.923)
3		1e-62	-1.445e+02	35.01%	21.03%	723.1bp (689.9bp)	Fli1(ETS)/CD8-FLI-ChIP-Seq(GSE20898)/Homer(0.910)
4		1e-59	-1.361e+02	25.31%	13.57%	676.0bp (658.0bp)	AT3G10030(Trihelix)/colamp-AT3G10030-DAP-Seq(GSE60143)/Homer(0.808)
5		1e-44	-1.035e+02	18.41%	9.54%	727.5bp (692.8bp)	CBF1(MacIsaac)/Yeast(0.874)
6		1e-34	-7.921e+01	45.00%	33.59%	626.8bp (808.8bp)	Sp1(Zf)/Promoter/Homer(0.890)
7		1e-30	-7.101e+01	19.54%	11.77%	911.0bp (413.8bp)	CEBP:AP1(bZIP)/ThioMac-CEBPb-ChIP-Seq(GSE21512)/Homer(0.956)
8		1e-29	-6.827e+01	15.72%	8.90%	783.8bp (645.1bp)	YY2/MA0748.1/Jaspar(0.850)
9		1e-23	-5.385e+01	31.12%	22.72%	696.8bp (816.3bp)	LARK(RRM,Znf)/Drosophila_melanogaster-RNCMPT00035-PBM/HughesRNA(0.931)
10		1e-22	-5.175e+01	20.57%	13.67%	851.3bp (457.7bp)	RUNX1(Runt)/Jurkat-RUNX1-ChIP-Seq(GSE29180)/Homer(0.971)
11		1e-19	-4.501e+01	38.17%	29.94%	686.3bp (703.1bp)	Lm_0254(RRM)/Leishmania_major-RNCMPT00254-PBM/HughesRNA(0.802)
12		1e-15	-3.614e+01	44.49%	36.86%	761.1bp (787.5bp)	CAT8/MA0280.1/Jaspar(0.791)
13 *		1e-11	-2.748e+01	34.31%	28.13%	612.3bp (835.5bp)	ERF094/MA1049.1/Jaspar(0.888)
14 *		1e-3	-8.086e+00	2.06%	1.25%	495.8bp (468.0bp)	MUB(KH)/Drosophila_melanogaster-RNCMPT00137-PBM/HughesRNA(0.891)

Gained MYB peaks

Rank	Motif	P-value	log P-pvalue	% of Targets	% of Background	STD(Bg STD)	Best Match/Details
1		1e-124	-2.875e+02	40.69%	10.49%	294.9bp (230.9bp)	GCN4/GCN4_SM/121-GCN4(Harbison)/Yeast(0.965)
2		1e-67	-1.563e+02	63.64%	35.29%	326.1bp (232.4bp)	PU.1(ETS)/ThioMac-PU.1-ChIP-Seq(GSE21512)/Homer(0.948)
3		1e-26	-6.129e+01	60.61%	42.91%	330.9bp (236.3bp)	ETV2/MA0762.1/Jaspar(0.806)
4		1e-22	-5.202e+01	35.82%	21.56%	317.4bp (225.7bp)	RUNX1(Runt)/Jurkat-RUNX1-ChIP-Seq(GSE29180)/Homer(0.969)
5		1e-18	-4.374e+01	31.39%	18.93%	432.0bp (229.6bp)	CEBPB/MA0466.2/Jaspar(0.918)
6		1e-16	-3.745e+01	24.68%	14.29%	379.6bp (230.5bp)	STZ(C2H2)/colamp-STZ-DAP-Seq(GSE60143)/Homer(0.788)
7 *		1e-6	-1.465e+01	11.69%	7.13%	307.8bp (237.9bp)	RPH1/Literature(Harbison)/Yeast(0.724)
8 *		1e-6	-1.464e+01	4.98%	2.19%	395.5bp (255.1bp)	gcm2/MA0917.1/Jaspar(0.733)
9 *		1e-5	-1.264e+01	9.09%	5.39%	363.4bp (259.0bp)	Rbm4.3(RRM)/Danio_rerio-RNCMPT00248-PBM/HughesRNA(0.798)
10 *		1e-5	-1.165e+01	11.26%	7.28%	645.5bp (244.4bp)	CMTA3/MA0970.1/Jaspar(0.797)
11 *		1e-4	-1.027e+01	10.28%	6.73%	346.2bp (227.8bp)	RPH1/MA0372.1/Jaspar(0.696)
12 *		1e-4	-9.924e+00	6.82%	4.03%	286.4bp (229.1bp)	PH0137.1_Pitx1/Jaspar(0.778)
13 *		1e-3	-7.136e+00	5.74%	3.61%	332.4bp (237.2bp)	MYB98(MYB)/col-MYB98-DAP-Seq(GSE60143)/Homer(0.877)
14 *		1e-2	-5.775e+00	2.71%	1.47%	776.4bp (245.6bp)	Vts1p(SAM)/Saccharomyces_cerevisiae-RNCMPT00111-PBM/HughesRNA(0.779)
15 *		1e-1	-4.352e+00	0.76%	0.27%	755.6bp (240.5bp)	ARF3/MA1009.1/Jaspar(0.759)
16 *		1e-1	-2.761e+00	0.97%	0.54%	589.8bp (238.8bp)	FXR2(KH)/Homo_sapiens-RNCMPT00020-PBM/HughesRNA(0.831)
17 *		1e0	-2.169e+00	1.95%	1.42%	591.0bp (222.8bp)	Optix/dmmpmm(Noyes_hd)/fly(0.822)

* possible false positive

Figure 6—figure supplement 1. CRYBMIM remodels MYB chromatin occupancies in AML cells. (**A–B**) Full lists of sequence motifs found in CRYBMIM-induced MYB-depleted (left) and MYB-enriched loci (right) after 1-hr treatment (**A**) and 4-hr treatment (**B**) of 20 μM CRYBMIM are shown.

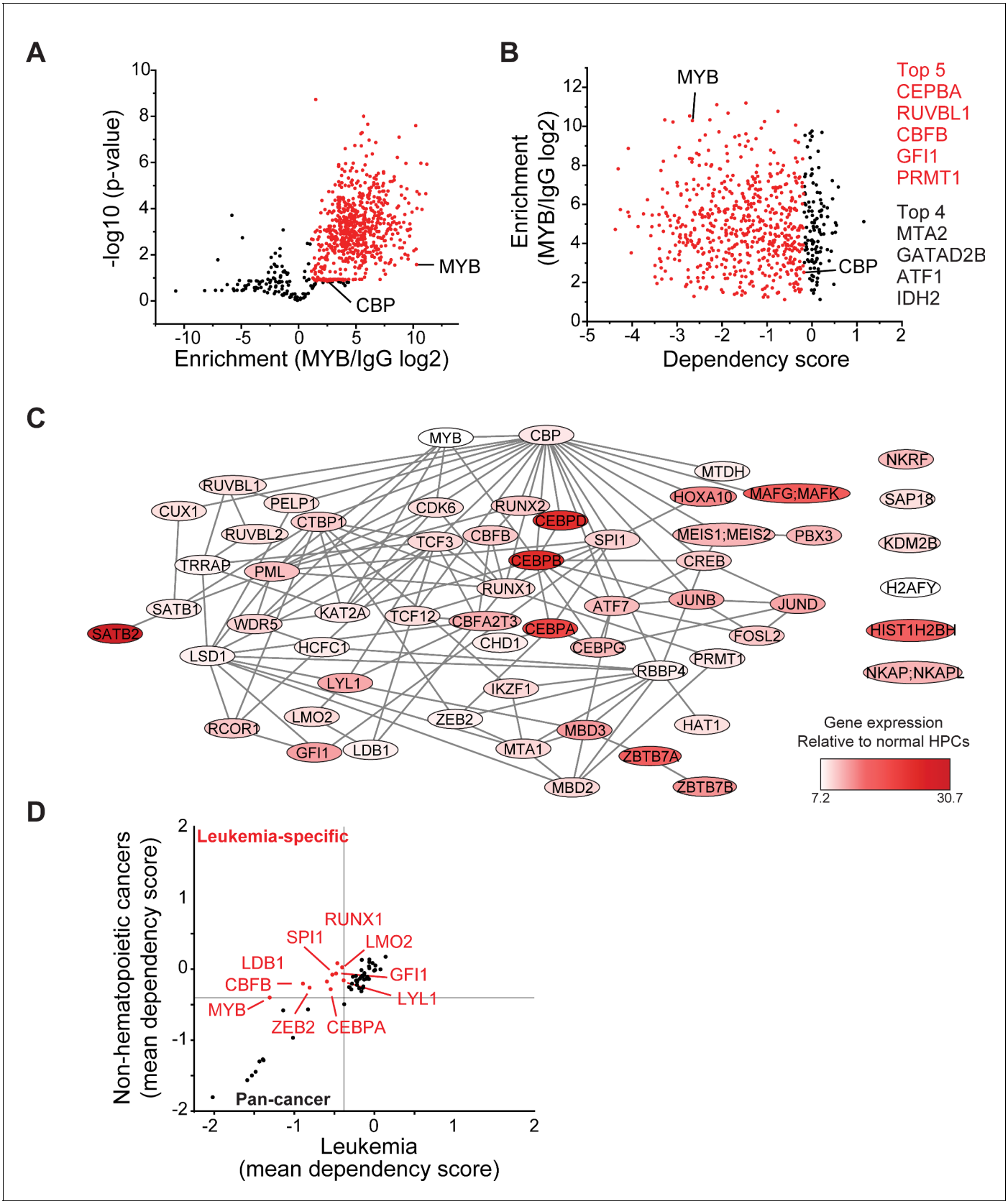

Figure 7. MYB assembles aberrant nuclear transcription factor complexes in AML cells. (**A**) Volcano plot of nuclear MYB-associated proteins compared to IgG control, as analyzed by affinity purification-mass spectrometry of MV411 cells. Red symbols denote specifically MYB-associated proteins, as

Figure 7 continued on next page

Figure 7 continued

defined by association with CBP (MYB/IgG $\log_2$ >1). p-Values denote statistical significance of three biological replicates. (**B**) Enrichment of MYB-associated proteins (red) as a function of their corresponding CRISPR DepMap dependency scores in MV411 cells. Red symbols denote functionally required proteins, as defined by the genetic dependency of CBP (score <−0.18). (**C**) Network of BioGRID protein interactions for MYB-associated nuclear AML proteins as a function of their respective hematopoietic expression aberrancy scores, based on their relative gene expression in AML cells as compared to normal bone human bone marrow progenitor cells (white to red color gradient indicates increasingly aberrant gene expression). (**D**) Comparison of the genetic dependency scores in leukemia cell lines as compared to all other non-hematopoietic cancer cell lines for MYB-associated nuclear AML proteins, with red symbols denoting proteins that are required in leukemia as compared to non-hematopoietic cancers.

Figure 7—figure supplement 1. CBP is the primary binding partner of MYB in AML cells. Sequence alignment of relevant CBP (top row) and P300 (bottom row) amino acids. Highlighted peptides identified in mass spectrometry analysis aligned to either CBP only (green) or both CBP and P300 (yellow).

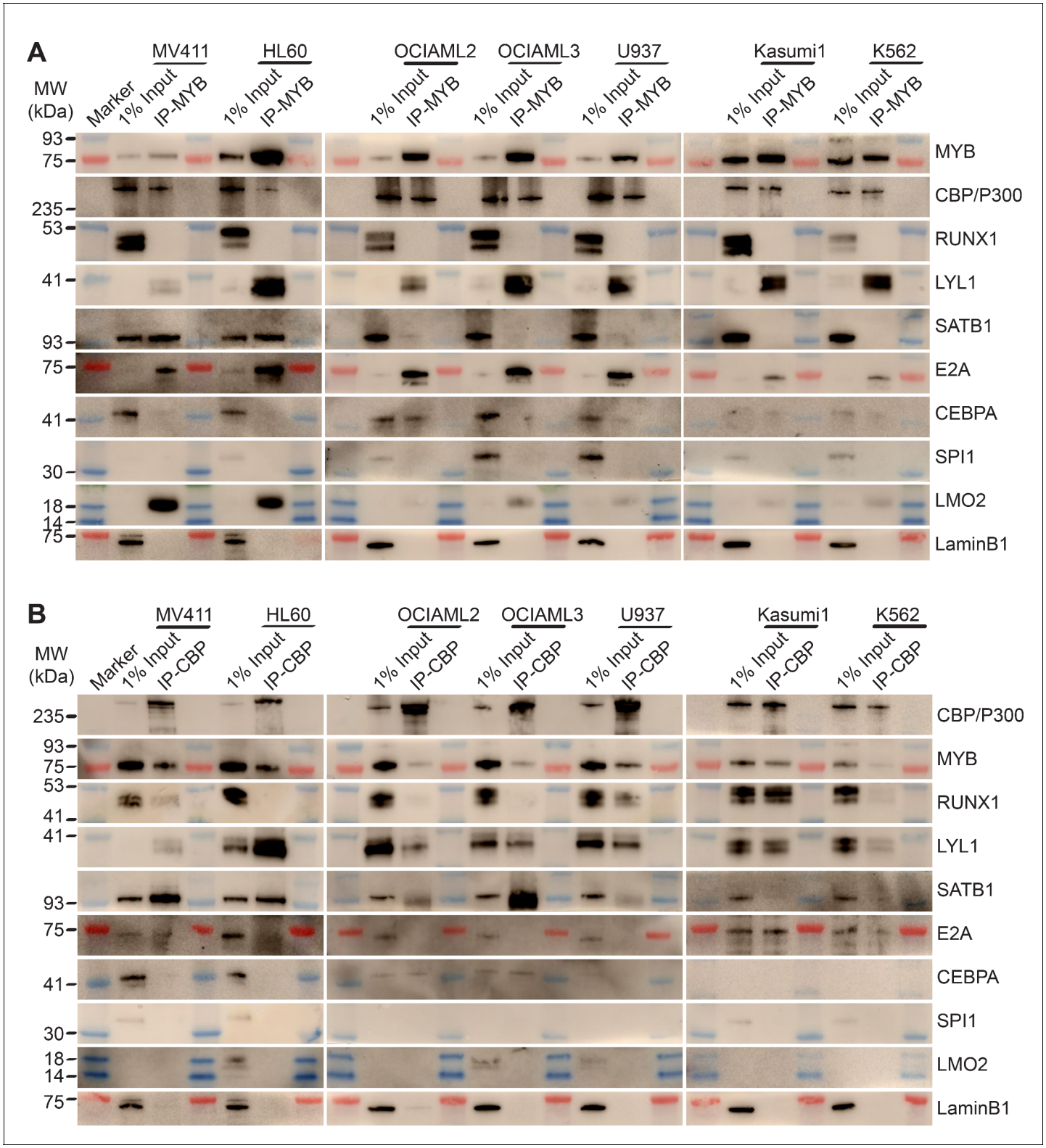

Figure 8. MYB and CBP/P300 assemble convergently organized nuclear transcription factor complexes in genetically diverse AML cells. (**A–B**) Western blots of specific transcription factors in immunoprecipitated MYB (**A**) and CBP/P300 (**B**) nuclear complexes in seven genetically diverse AML cell lines, as indicated. Blue and red bands indicate molecular weight markers. LaminB1 serves as the loading control.

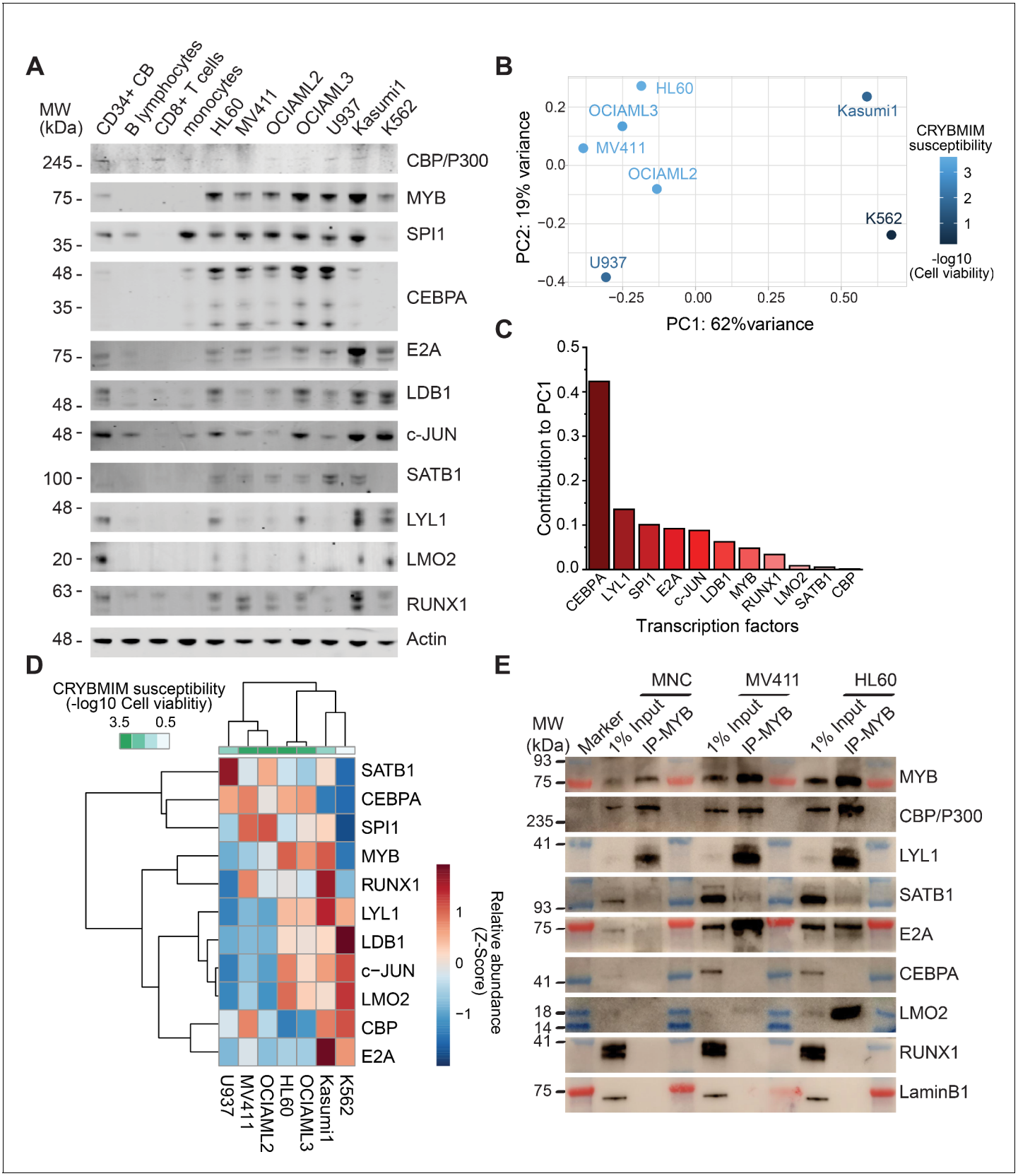

Figure 9. Specific MYB complex factors are aberrantly expressed and assembled in AML as compared to normal human blood cells. (**A**) Western blots of specific MYB complex transcription factors in normal human blood cells and genetically diverse leukemia cells, as indicated. Actin serves as the

Figure 9 continued on next page

Figure 9 continued

loading control. (**B**) Principal component analysis of MYB complex transcription factor abundance, as quantified by image densitometry, as a function of susceptibility of various AML cell lines to CRYBMIM (blue color index). (**C**) Contribution of individual MYB complex transcription factor abundance to the top PCA eigenvector. (**D**) Heatmap of hierarchical clustering of MYB complex individual transcription factor abundance and CRYBMIM susceptibility. (**E**) Western blots of specific transcription factors in specific MYB nuclear complexes immunoprecipitated from normal human umbilical cord mononuclear cells (MNC), as compared to MV411 and HL60 AML cells. Blue and red bands indicate molecular weight markers. LaminB1 serves as loading control.

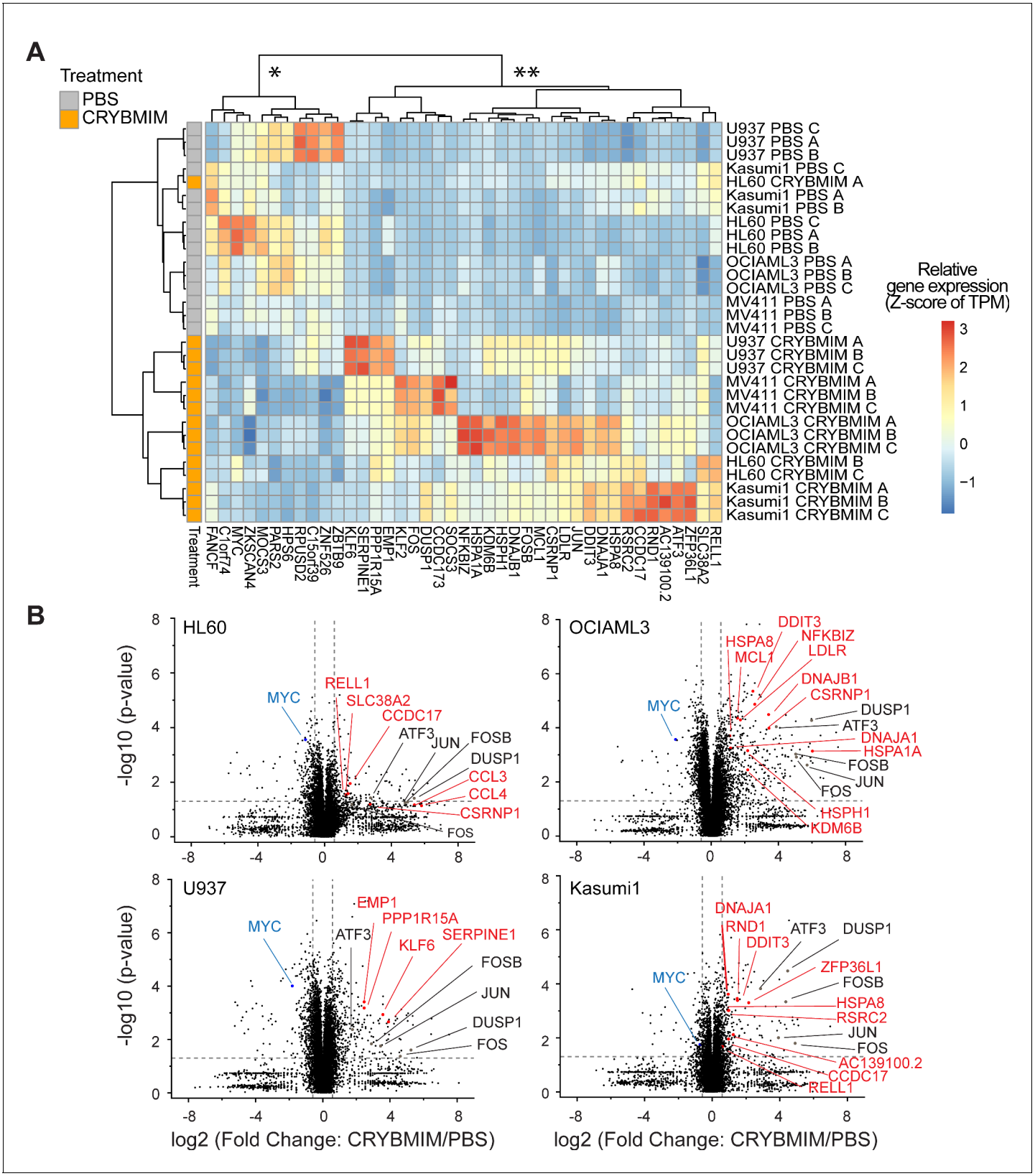

Figure 9—figure supplement 1. MYB transcription complexes induce shared and repress distinct gene expression programs in genetically diverse AML cells, as remodeled by peptidomimetic CRYBMIM inhibition. (**A**) Gene expression of five genetically diverse AML cell lines treated with 20 μM CRYBMIM (brown) as compared to PBS control (gray) for 1 hr, and measured by transcriptome RNA sequencing. Blue to red color gradient denotes

Figure 9—figure supplement 1 continued on next page

Figure 9—figure supplement 1 continued

relative gene expression of transcripts per million reads (TPM). Unsupervised clustering demonstrates gene sets that are repressed (*) and induced (**) by CRYBMIM and are shared and distinct among diverse AML cell lines, respectively, with top differentially expressed genes labeled. Data represent biological triplicates (**A, B, C**). (**B**) Volcano plots of differentially expressed genes following treatment with 20 μM CRYBMIM for 1 hr in genetically diverse AML cell lines. Vertical dashed lines denote relative changes in transcript abundance, and horizontal dashed line denotes statistical significance of biological triplicates (p=0.05).

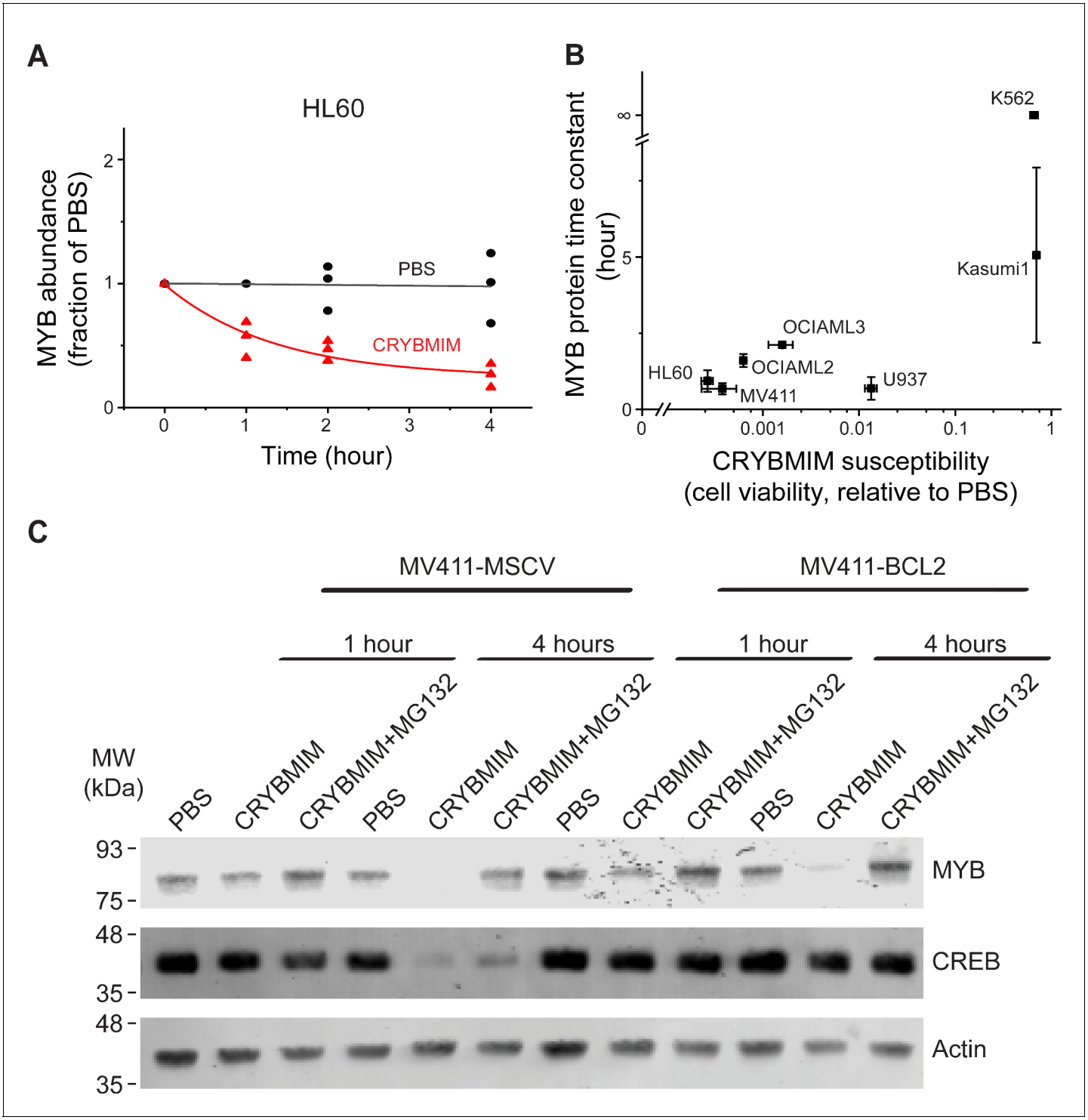

Figure 10. Peptidomimetic remodeling of MYB transcriptional complexes leads to rapid MYB proteolysis. (**A**) Quantification of MYB abundance in HL60 cells as a function of duration of 20 μM CRYBMIM treatment (red) as compared to PBS control (black) using Western blot image densitometry. Lines represent single exponential decay fits. Western blots and fits for all cell lines studied are shown in ***Figure 10—figure supplement 1***. Symbols represent biological triplicates. (**B**) MYB protein half-life, as estimated by exponential decay kinetics, in genetically diverse AML cell lines as a function of CRYBMIM susceptibility (Pearson $r = 0.94$, excluding resistant K562). Horizontal bars represent standard deviation of CRYBMIM susceptibility. Vertical bars represent standard deviation of time constants. (**C**) Western blots of MYB and CREB in MV411 AML cells transduced with MSCV retroviruses encoding *GFP* control (MV411-MSCV) or *BCL2* (MV411-BCL2), treated with 20 μM CRYBMIM or PBS control with or without 10 μM of MG132 for 1 or 4 hr, as indicated. Actin serves as loading control.

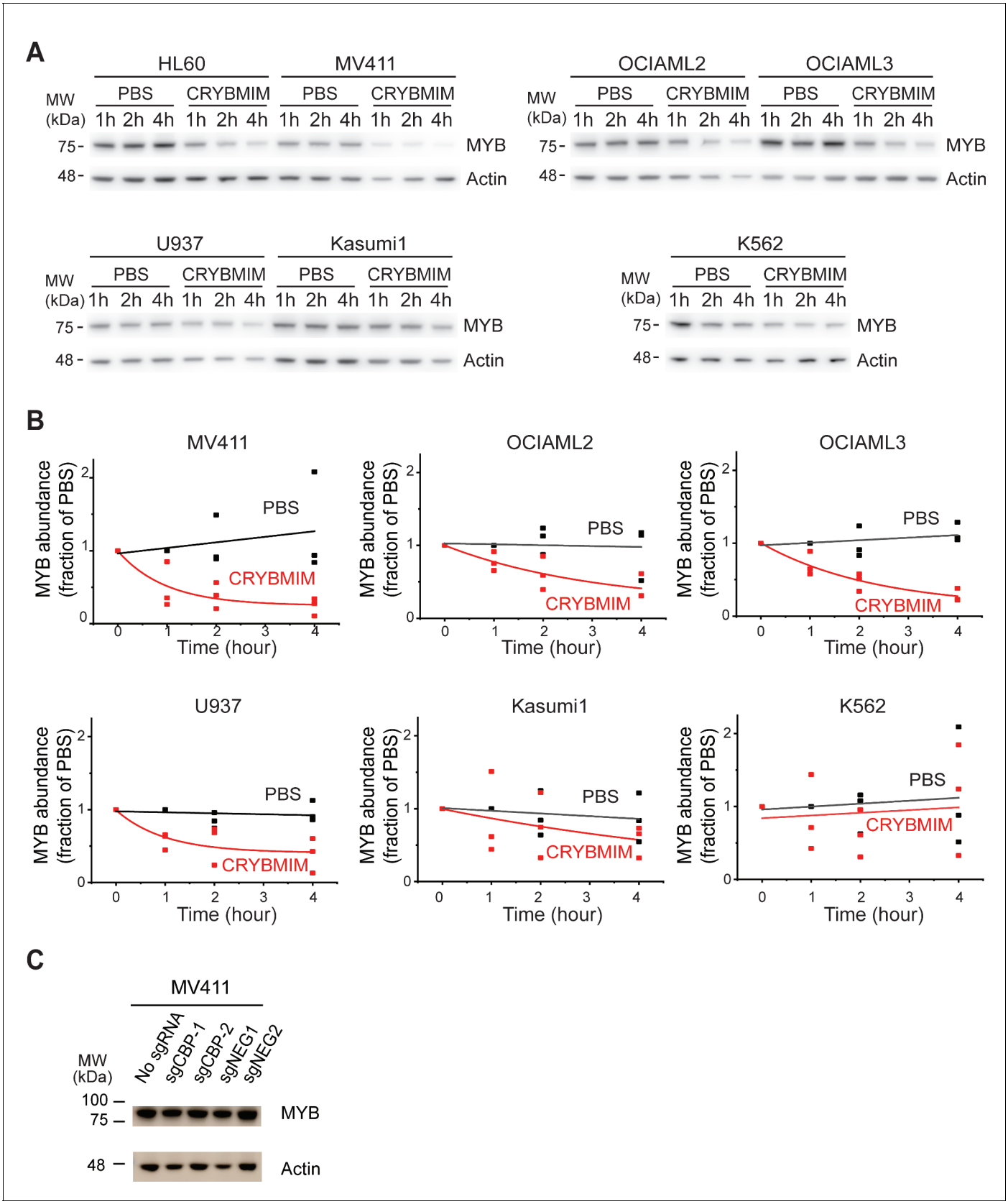

Figure 10—figure supplement 1. CRYBMIM causes MYB proteolysis with differential degradation rates in AML cells. (**A–B**) Western blots (**A**) and quantification of MYB protein abundance (**B**) in AML cells upon 1, 2, or 4 hr of 20 μM CRYBMIM (red) or PBS (black) treatment using image

Figure 10—figure supplement 1 continued on next page

Figure 10—figure supplement 1 continued

densitometry. Lines indicate single exponential fits. Actin serves as loading control. (**C**) Western blots demonstrating MYB protein abundance in MV411 cells expressing sgCBP-1 and sgCBP-2 as compared to control sgNEG1 and sgNEG2. Actin serves as the loading control.

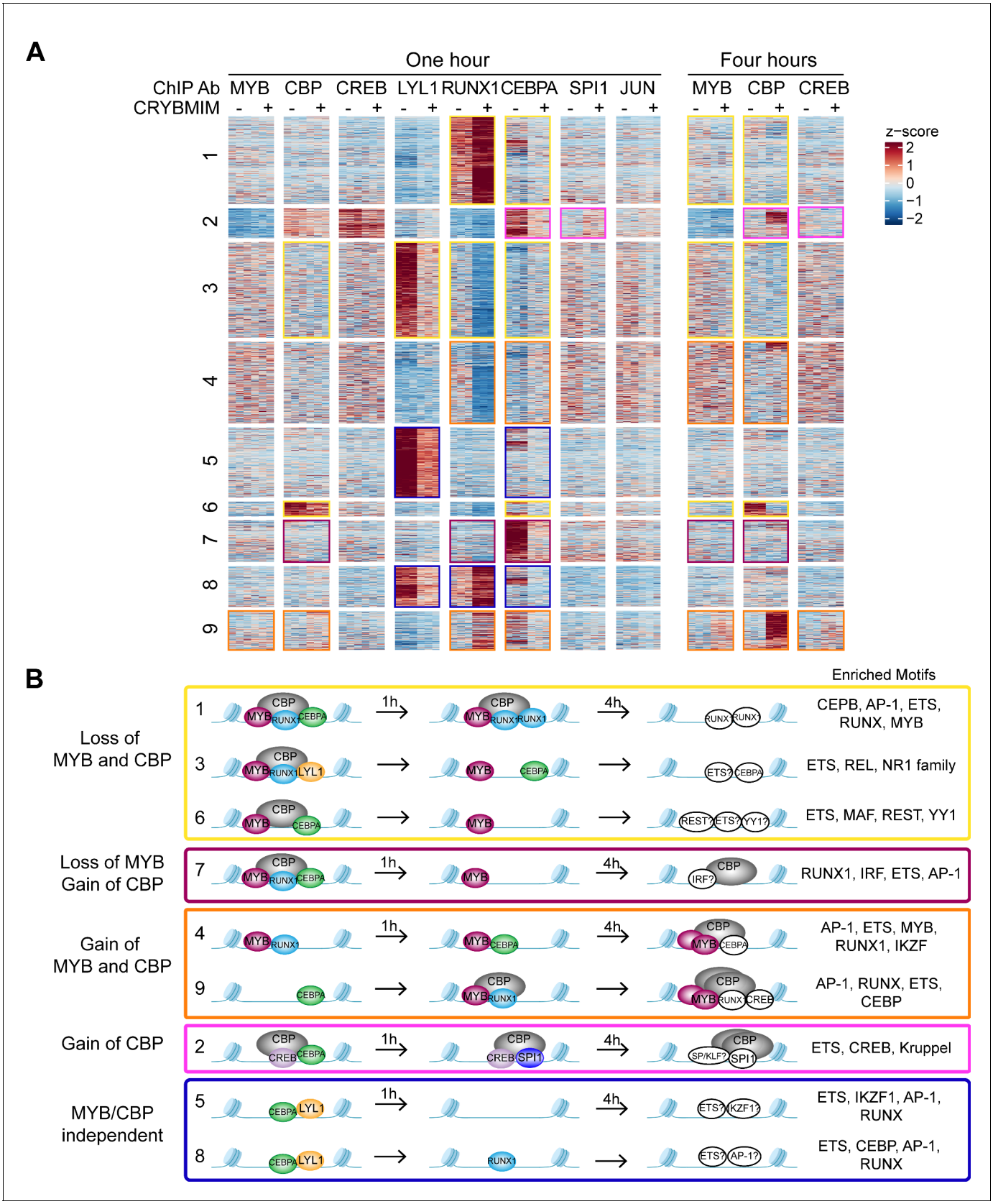

Figure 11. Chromatin dynamics of CRYBMIM remodeled MYB transcription factor complexes in AML cells. (**A**) Heatmap of transcription factor chromatin occupancy in MV411 cells as a function of time of control PBS or CRYBMIM treatment. Nine clusters identified using k-means clustering are

Figure 11 continued on next page

Figure 11 continued

marked by yellow (loss of MYB and CBP), purple (loss of CBP and gain of MYB), orange (gain of MYB and CBP), pink (gain of CBP), and blue (no apparent changes of MYB and CBP) boxes, based on the similarity of their *z*-scores, with red and blue representing enrichment or depletion of factors, respectively. (**B**) Groups of clusters comprising similar responses to CRYBMIM treatment based on MYB and CBP/P300 dynamics. Sequence motifs enriched at specific loci for each cluster are listed. Factors in white denote factors presumed to be enriched based on sequence motif enrichment.

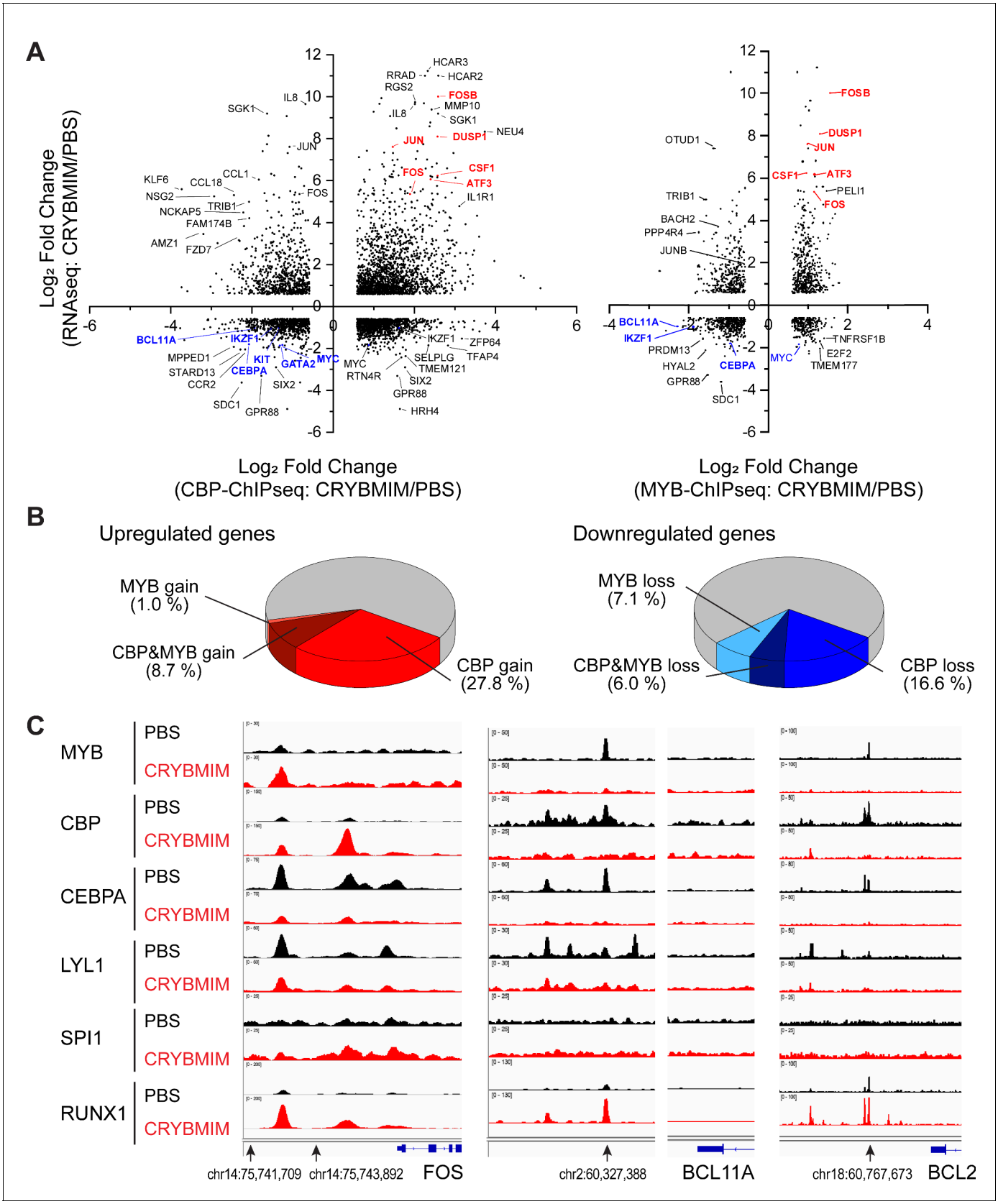

Figure 11—figure supplement 1. Oncogenic MYB transcription complexes sequester CBP/P300 to control AML gene expression. (**A**) Relative gene expression as measured by transcriptome RNA-seq as a function of relative chromatin occupancy of CBP/P300 (left) and MYB (right) as measured by

Figure 11—figure supplement 1 continued on next page

Figure 11—figure supplement 1 continued

ChIP-seq in MV411 cells treated with 20 μM CRYBMIM versus PBS control for 4 hr. Genes are labeled for greatest peak fold change >1.5 and FDR < 0.1. (**B**) Distribution of upregulated (left) and downregulated (right) genes with respect to the relative gain (red) and loss (blue) chromatin occupancy of CBP/P300 and MYB. (**C**) Chromatin occupancy of specific factors in *FOS* (left), *BCL11A* (middle), and BCL2 (right) loci that are upregulated, downregulated and not changed, respectively, upon CRYBMIM (red) as compared to PBS control (black) treatment.

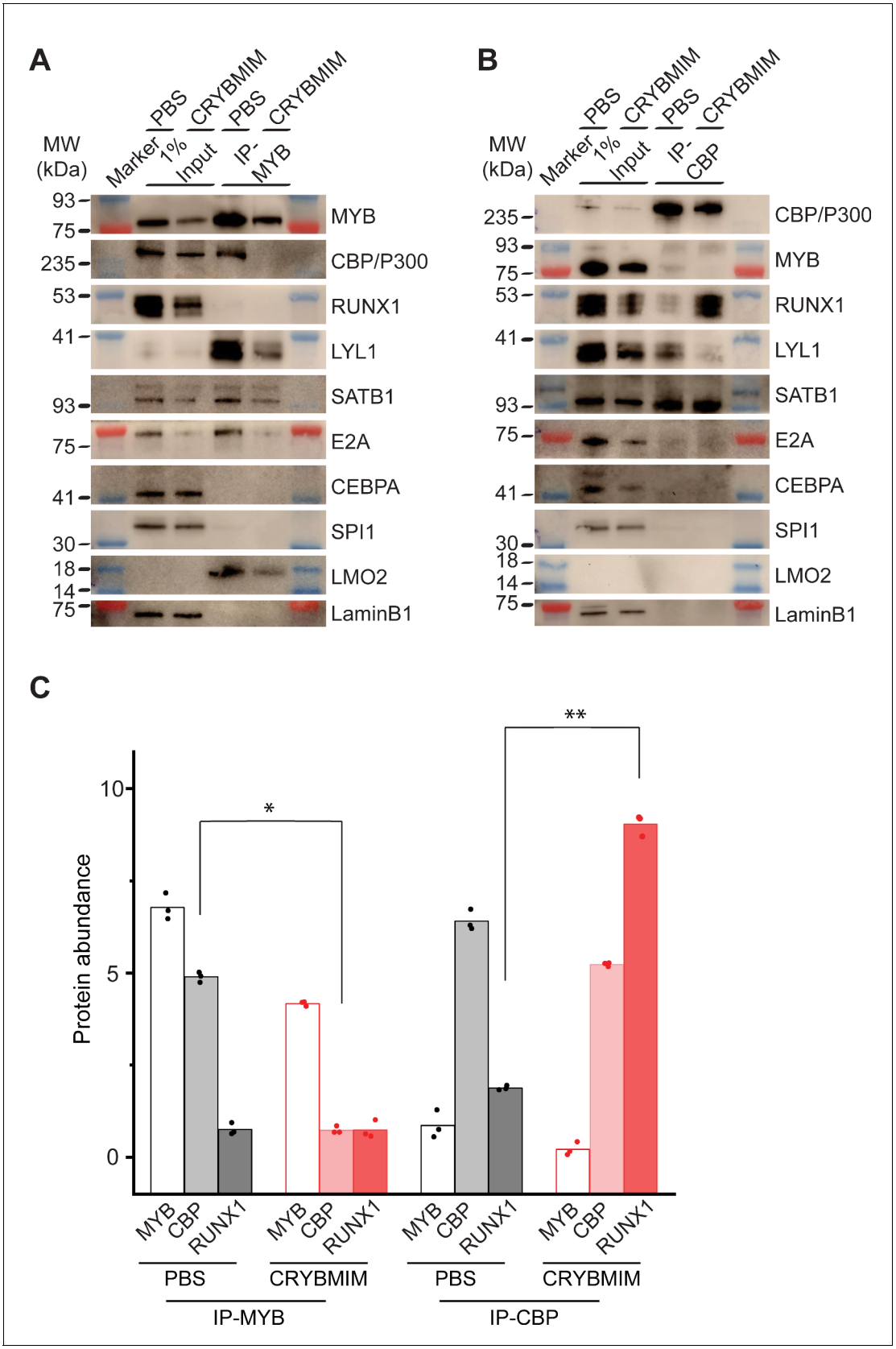

Figure 12. Peptidomimetic blockade of MYB:CBP/P300 by CRYBMIM releases CBP/P300 that recruits RUNX1 to chromatin. (**A–B**) Western blots of specific transcription factors in nuclear complexes with immunoprecipitated MYB (**A**) and CBP/P300 (**B**) in MV411 cells upon treatment with 10 μM

Figure 12 continued on next page

Figure 12 continued

CRYBMIM or PBS control for 1 hr. Blue and red bands indicate molecular weight markers. LaminB1 serves as loading control. (**C**) Abundance of MYB, CBP/P300 and RUNX1, as measured by western blot image densitometry, in immunoprecipitated MYB and CBP/300 nuclear complexes in MV411 cells treated with CRYBMIM or PBS control. Symbols represent biological triplicates; *p=4.7e-6, t-test for CBP in MYB complex upon CRYBMIM treatment, **p=3.4e-6, t-test for RUNX1 in CBP/P300 complex CRYBMIM treatment.

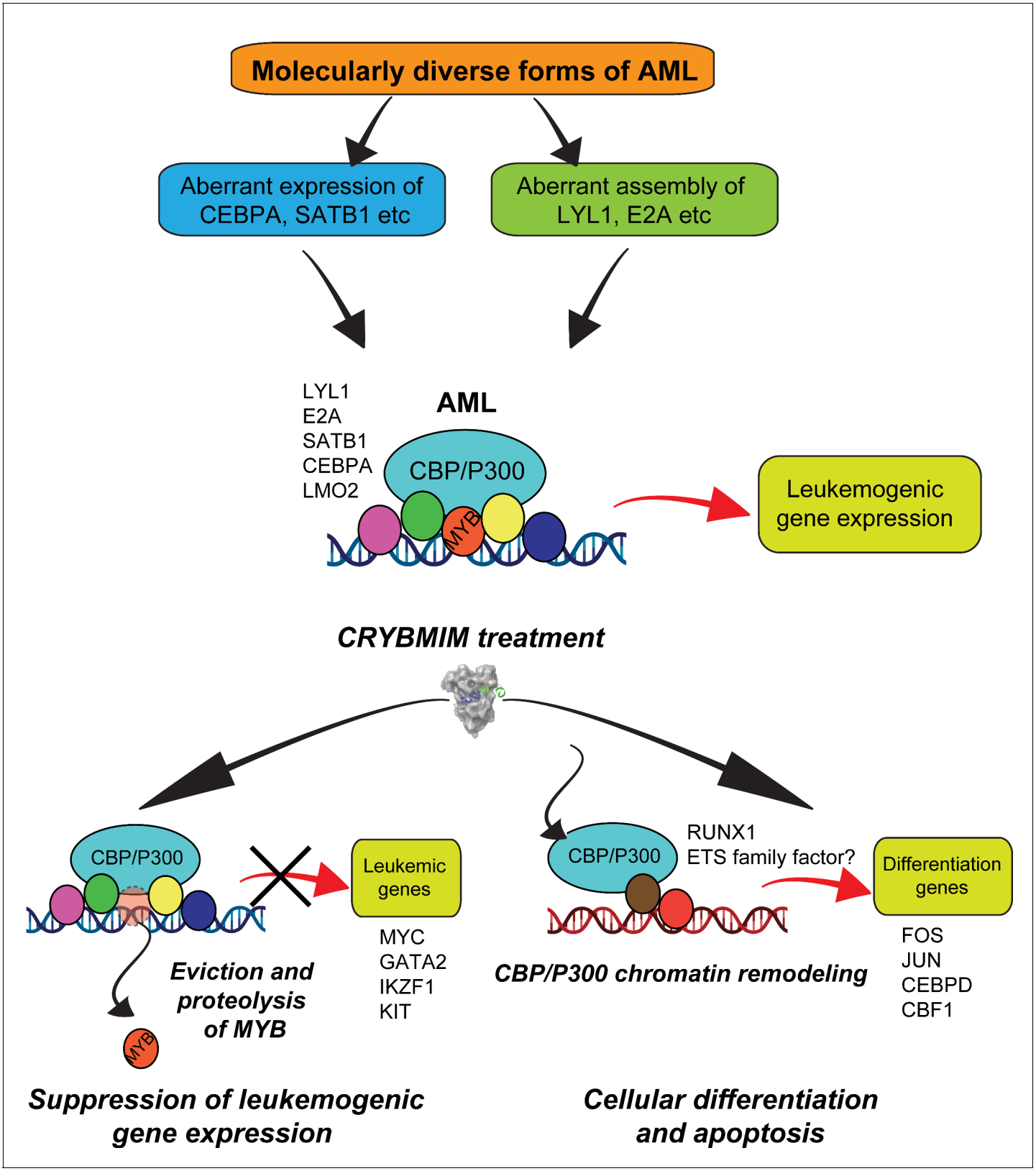

Figure 13. Convergent organization of aberrant MYB complexes controls oncogenic gene expression in acute myeloid leukemia. Schematic of the molecular organization of MYB transcription factor complexes, induced convergently in genetically diverse subtypes of AML, leading to oncogenic gene expression that requires MYB:CBP/P300 interaction and causes susceptibility to its peptidomimetic remodeling, leading to MYB chromatin eviction and proteolysis, and CBP/P300 release to induce cellular differentiation and apoptosis.